Stepwise evolution of *E. coli* C and ΦX174 reveals unexpected lipopolysaccharide (LPS) diversity

Jordan Romeyer Dherbey[1]*, Lavisha Parab[1], Jenna Gallie[2], and Frederic Bertels[1]*

[1]Department Microbial Population Biology, Research Group Microbial Molecular Evolution, Max Planck Institute for Evolutionary Biology, Plön (24306), Germany

[2]Department for Evolutionary Theory, Research Group Microbial Evolutionary Dynamics, Max Planck Institute for Evolutionary Biology, Plön (24306), Germany

*Corresponding authors:

Jordan Romeyer Dherbey. Address: Max Planck Institute for Evolutionary Biology, August-Thienemann-Straße 2, 24306 Plön, Germany; email: dherbey@evolbio.mpg.de; phone: + 49 4522 763-278. ORCID 0000-0002-6125-1722.

Frederic Bertels. Address: Max Planck Institute for Evolutionary Biology, August-Thienemann-Straße 2, 24306 Plön, Germany; email: bertels@evolbio.mpg.de; phone: + 49 4522 763-222. ORCID 0000-0001-6222-4139.

Preprint server: https://www.biorxiv.org/content/10.1101/2022.09.06.506728v1. The copyright holder for this preprint is the author/funder, who has granted bioRxiv a license to display the preprint in perpetuity. It is made available under a CC-BY 4.0 International license.

Classification: Biological Sciences, Evolution

Keywords: LPS, Overcoming host resistance, Genotype-phenotype maps, Experimental evolution, ΦX174, *E. coli* C.

Abstract

Phage therapy is a promising method for the treatment of multi-drug-resistant bacterial infections. However, its long-term efficacy depends on understanding the evolutionary effects of the treatment. Current knowledge of such evolutionary effects is lacking, even in well-studied systems. We used the bacterium *Escherichia coli* C and its bacteriophage ΦX174, which infects cells using host lipopolysaccharide (LPS) molecules. We first generated 31 bacterial mutants resistant to ΦX174 infection. Based on the genes disrupted by these mutations, we predicted that these *E. coli* C mutants collectively produce eight unique LPS structures. We then developed a series of evolution experiments to select for ΦX174 mutants capable of infecting the resistant strains. During phage adaptation, we distinguished two types of phage resistance: one that was easily overcome by ΦX174 with few mutational steps ("easy" resistance), and one that was more difficult to overcome ("hard" resistance). We found that increasing the diversity of the host and phage populations could accelerate the adaptation of phage ΦX174 to overcome the hard resistance phenotype. From these experiments, we isolated 16 ΦX174 mutants that, together, can infect all 31 initially resistant *E. coli* C mutants. Upon determining the infectivity profiles of these 16 evolved phages, we uncovered 14 distinct profiles. Given that only eight profiles are anticipated if the LPS predictions are correct, our findings highlight that the current understanding of LPS biology is insufficient to accurately forecast the evolutionary outcomes of bacterial populations infected by phage.

Introduction

Multidrug-resistant bacterial infections are one of the most pressing issues in medicine, a situation that is only expected to worsen in the coming decades (Centers for Disease Control and Prevention (U.S.) 2019; WHO 2021; Murray et al. 2022). An alternative to treating bacterial infections with antibiotics is phage therapy. Major research efforts are being conducted to develop efficient therapies (Oechslin 2018; Bull et al. 2019; Monteiro et al. 2019). An efficient therapy should be able to eliminate a pathogen without selecting for resistance to the phage being used to treat that pathogen. Phage resistance can often evolve by modifying the cell envelope to avoid phage adsorption. The outer membrane of all Gram-negative bacteria is covered in lipopolysaccharides (LPSs), which is consequently the first contact point between a bacterium and its environment (Zhang et al. 2013). LPS structure determines whether a bacterium will be recognized by the immune system, the efficiency of nutrient uptake as well as the susceptibility to antibiotics and, importantly, the susceptibility to phage infection (Nikaido 2003; Simpson and Trent 2019; Mutalik et al. 2020). Hence, LPS structure is an important factor determining the success of phage therapy.

The functions of genes involved in synthesizing and assembling bacterial LPS have been elucidated (Schnaitman and Klena 1993; Amor et al. 2000; Raetz and Whitfield 2002; Qian et al. 2014; Klein and Raina 2019). Most *Escherichia coli* strains produce LPS molecules composed of three parts: the lipid A, the core oligosaccharide (OS), and the O-antigen chain. The LPS core OS itself consists of a very conserved inner core across *E. coli* species and a variable outer core (Amor et al. 2000). Strains with the tripartite LPS molecules (lipid A, core OS, and O-antigen) are termed "smooth" (Raetz and Whitfield 2002). Some *E. coli* strains, however, produce LPS molecules that lack one or more components. LPS molecules lacking the O-antigen are classified as "rough", and molecules lacking both the O-antigen and the outer core OS as "deep rough" (van der Ley et al. 1986; Schnaitman and Klena 1993; Yethon et al. 1998; Whitfield et al. 1999; Amor et al. 2000; Klein et al. 2013). These modifications in LPS structure can lead to a plethora of phenotypic effects (Simpson and Trent 2019), including (i) destabilization of the outer membrane (Raetz and Whitfield 2002), (ii) changes in the expression of some outer membrane proteins, (iii) modification of intracellular turgor pressure (Pagnout et al. 2019), (iv) increased susceptibility to hydrophobic compounds such as antimicrobial peptides, antibiotics, and bacteriocins (van der Ley et al. 1986; Schnaitman and Klena 1993; Yethon et al. 1998; Whitfield et al. 1999; Amor et al. 2000; Klein et al. 2013), (v) altered interactions with the

host immune system (Raetz and Whitfield 2002; Matsuura 2013; Maldonado et al. 2016), (vi) alteration of the redox status of cells leading to oxidative stress (Seregina et al. 2022), and (vii) changes in resistance to phages (Hancock and Reeves 1976; Labrie et al. 2010; Kulikov et al. 2019; Mutalik et al. 2020).

Phage ΦX174 is a small (~320 Å), tailless, lytic coliphage from the *Microviridae* family. It carries a circular, single-stranded DNA genome of only 5386 bases long that encodes 11 genes (Sinsheimer 1959; Sanger et al. 1978). To enter a host cell, ΦX174 relies solely on attaching to the core OS by one of its spike proteins before migrating and irreversibly adsorbing to the host's cell surface via its capsid (Incardona and Selvidge 1973; Incardona et al. 1985; Sun et al. 2017). ΦX174 does it with a high degree of specificity. For instance, among 783 different *E. coli* isolates, only six (0.8 %) could be infected by wildtype ΦX174 (Michel et al. 2010). In the laboratory, ΦX174 infects - and hence is usually grown on - *E. coli* C, which produces rough type (*i.e.*, lacking in O-antigen) LPS molecules (Feige, Ulrich and Stirm, Stephan 1976; Inagaki et al. 2000; Kawaura et al. 2000; Król et al. 2019) (**Figs. 1 and S1**).

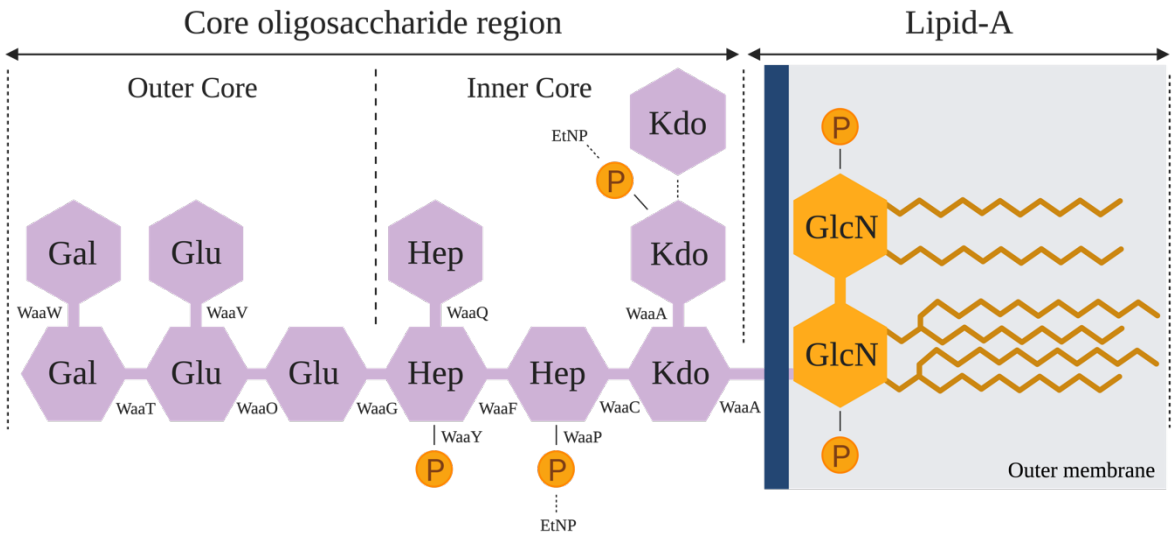

Fig. 1. Structure of *E. coli* C's rough type LPS. The rough type LPS of *E. coli* C is composed of two parts: lipid A (composed of an acetylated and 1,4'-diphosporylated β(1→6)-linked glucosamine (GlcN) disaccharide), and the core oligosaccharide (Raetz and Whitfield 2002). The core oligosaccharide is subdivided into a structurally conserved inner core and an outer core. The dashed lines show non-stochiometric substitutions of phosphate (P), ethanolamine (EtNP), and 3-deoxy-D-

102 *manno*-octulosonic acid (Kdo) residues on the LPS (Kojima et al. 2010). Details of the LPS assembly
103 process are provided in **Fig. S1**.
104
105 Here, we explore the evolutionary potential of *E. coli* C to become resistant to infection by ΦX174
106 and, conversely, the potential of ΦX174 mutants to infect phage-resistant *E. coli* C hosts with modified
107 LPS structures. We first generated a set of 31 *E. coli* C mutants that are resistant to infection by ΦX174
108 wildtype and determined that each mutant carries at least one mutation affecting LPS biosynthesis.
109
110 The currently accepted model for predicting LPS structure posits that the presence or absence of each
111 LPS gene leads to a single LPS phenotype. Based on the position of each mutation, the one-gene-one-
112 phenotype model allows us to predict the LPS structure of each of our LPS mutants. Our 31 *E. coli* C
113 mutants collectively produce LPS molecules with eight distinct structures. To test the accuracy of
114 these predictions, we evolved and genotypically characterized a set of 16 ΦX174 genotypes that can,
115 together, infect all initially resistant 31 *E. coli* C mutants. If the LPS structure predictions are correct,
116 then all bacteria predicted to carry the same LPS structure should be susceptible to the same set of
117 phages. Interestingly, this was not always the case, indicating that the diversity of LPS structures
118 generated by LPS-pathway mutations is much higher than anticipated from previous studies. Bacterial
119 strains with different mutations in the same LPS gene sometimes have strikingly different infection
120 phenotypes. Even the required number of phage mutations to overcome these resistances can differ
121 significantly. A better understanding of the evolution of phage resistance hence requires a better
122 understanding of the biology and evolution of LPS structures.
123

124 ## Results

125 ### Diverse LPS structures confer resistance to ΦX174 infection

126 To study LPS diversity in *E. coli* C, we generated 35 spontaneous phage-resistant strains and used
127 whole genome re-sequencing to identify the mutations conferring resistance (see **Methods**). Due to a
128 lack of isogeneity or only partial resistance to wildtype ΦX174, four of these strains (*E. coli* C R1, R3,
129 R15, and R19) were excluded from downstream analyses (see **Text S1**). Of the remaining 31 strains,
130 27 are predicted to carry a single mutation, three carry two mutations, and one carries three mutations
131 (see **Table S1**). A total of 36 mutations were identified, 32 of which are unique (including 15 nucleotide
132 substitutions, 13 deletions, one duplication, and three IS*4* and IS*5* insertion events). Twenty-four (of

133 32, or 75%) mutations introduce premature stop codons or lead to frameshifts and thus are highly
134 likely to disrupt gene function.
135
136 Interestingly, two mutations are shared by two strains (R27/R31 and R8/R10), and one mutation is
137 shared by three strains (R4/R24/R29). Given that there are almost limitless ways to disrupt gene
138 function, this high degree of parallelism is initially surprising. We note that the repetition of these
139 mutations is unlikely to result from their positive selection. That is, phage-resistant *E. coli* C mutants
140 of both low and high fitness are expected to have an equal chance of appearing on our agar plates as
141 long as they can form visible colonies (Luria and Delbrück 1943). Presumably, the observed parallelism
142 is, instead, due to elevated mutation rates at particular genomic positions (Lind et al. 2019). The fact
143 that two of three parallel mutations occur in homopolymeric tracts supports this hypothesis (Moxon
144 et al. 1994).
145
146 Mutations in genes encoding the LPS machinery are expected to lead to changes in LPS structure and,
147 in some cases, a switch from a rough to a deep rough phenotype (Yethon et al. 1998; Whitfield et al.
148 1999; Yethon et al. 2000). It has been shown that logical predictions of mutant LPS structures can be
149 made. If an enzyme that synthesizes a particular LPS component is absent or non-functional, then
150 that LPS component cannot be synthesized. In addition, LPS components assembled downstream of
151 the missing component are also absent from the final LPS structure. The assumption that each
152 mutation in an LPS gene leads to a complete lack of function allows us to predict the LPS structure
153 and type of each of the 31 *E. coli* C phage-resistant mutants (**Figs. 2**, **S1**, **S2 and Table S1**). A total of
154 seven emergent LPS structures were predicted from our set of mutants (**Fig. 2**). Compared with the
155 *E. coli* C wildtype LPS, three of these seven LPS structures carry alterations in the outer-core LPS and
156 hence are predicted to be of the rough type (as is wildtype *E. coli* C; ten mutants). The remaining four
157 LPS structures differ from wildtype LPS in both the inner- and outer-core LPS, and are presumed to
158 be of the deep rough type (twenty mutants) (see **Table S1**).
159
160 The LPS structure and type of the remaining mutant (*E. coli* C R25) were not predicted because the
161 effect of the phage-resistance mutation on LPS biosynthesis remains unclear. R25 carries a nonsense
162 mutation in *rfaH*. The *rfaH* gene encodes a transcriptional antiterminator that regulates the *waa* operon
163 (Bailey et al. 1997; Klein and Raina 2019), meaning that any number of LPS biosynthetic genes could
164 potentially be affected by this mutation.

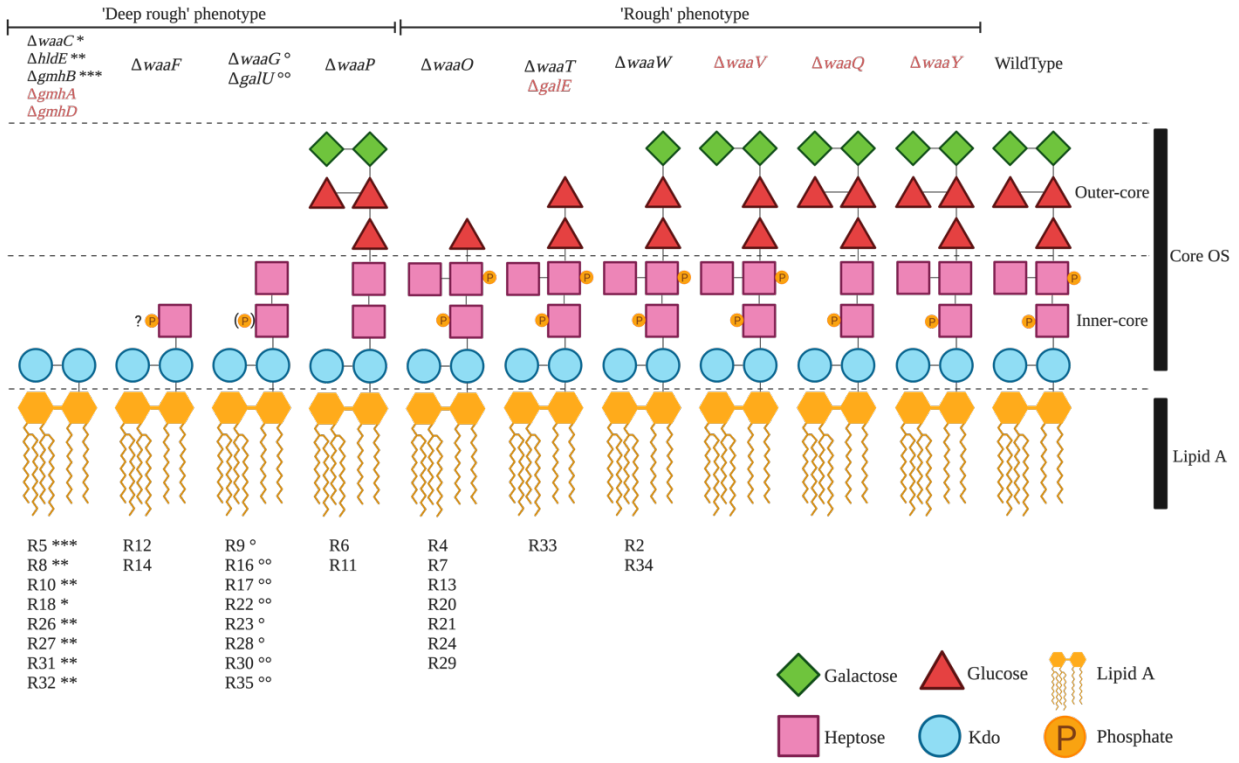

Fig. 2. Predicted LPS structures of 30 ΦX174-resistant *E. coli* C strains. Predicted LPS structures fall into two groups depending on their degree of truncation and/or loss of phosphate groups: the "deep rough" phenotype with a completely truncated outer core or a loss of phosphate groups (twenty *E. coli* C mutants) and the "rough" phenotype with smaller LPS truncations located in the outer core (ten *E. coli* C mutants). The LPS phenotype of the final *E. coli* C mutant (R25) could not be predicted (see text). The products of genes in red are also involved in LPS biosynthesis and, although no mutations were identified in these genes during this study, are also potential targets for phage resistance. Details on the functions of *gmhA*, *gmhB*, *gmhD*, *hldE*, *galU*, and *galE* are provided in **Fig. S2**. "?P": No information was found on the phosphorylation of Hep(I) in the absence of *waaF*; (P): only 40% of the hexose phosphorylation was observed (Yethon et al. 2000); R#: the number gave to each *E. coli* C resistant strain; "*, **, ***, °, °°": symbols link the resistant strains (R#) to particular mutated LPS genes (Δ*gene-names*). Resistant strains with identical symbols carry their mutations in the same LPS gene. For example, [R8, R10, R26, R27, R31, and R32]-strains each carry a mutation in the *hldE* gene, and [R9, R23, and R28]-strains all carry a mutation in the *waaG* gene (**Table S1**).

183 The LPS structure predictions above can be tested by evolving wildtype ΦX174 to specifically infect
184 *E. coli* C cells with modified LPS structures. That is, a phage that can infect a given modified LPS
185 structure is expected to be able to infect all bacterial strains displaying this LPS type, regardless of the
186 underlying mutations. Alternatively, the inability of mutant phages to cross-infect bacterial strains of
187 the same predicted LPS structural class (but via different mutations) would indicate that these
188 mutations actually lead to distinct LPS structures.
189
190 **ΦX174 evolves to overcome host resistance, a process that can be accelerated by host diversity**
191 Phages that can infect resistant *E. coli* C mutants were evolved by serially transferring wildtype ΦX174
192 on each of the 31 resistant *E. coli* C strains (**Fig. 3A and Methods**). To reduce the complexity of the
193 experiment, bacterial cultures were not allowed to co-evolve. Instead, phages were inoculated into
194 fresh, exponentially growing host cultures at each transfer. The experiment gave rise to 12 evolved
195 phages that were collectively able to infect 21 (of the 31) initially resistant *E. coli* C strains (these display
196 the "easy" resistant phenotype; see **Table S1**). However, even after 21 transfers, ten (of 31) resistant
197 *E. coli* C strains remained uninfected (the "hard" resistant phenotype; see **Table S1**).
198
199 Overcoming phage resistance of this subset of hard-resistant strains may not be achievable with few
200 mutational steps. Hence, either the evolution experiment has to be performed for a much longer
201 period of time, or an experiment that increases the genetic variation available to evolution has to be
202 designed (Hermisson and Pennings 2005; Barrett and Schluter 2008). We designed two further
203 evolution experiments, one to increase genetic diversity and another one to additionally increase the
204 speed of evolution by increasing the number of phage generations per day (**Figs. 3B and 3C**). In both
205 of these experiments, phage diversity was increased by combining all evolved phage strains that
206 successfully reinfected their corresponding resistant strains into a single phage cocktail (Hermisson
207 and Pennings 2005; Barrett and Schluter 2008). The phage cocktail was serially transferred once per
208 day in the overall second evolution experiment, while four transfers per day were performed in the
209 third evolution experiment. Phage diversity was maintained from one transfer to another by adding
210 all corresponding resistant strains to the host culture (see **Methods**). At the end of the evolution
211 experiments, all resistant strains could be cross-infected by at least one of the evolved phage mutants.
212 Our method of evolving phages with an extended infection range is simple and effective and allows
213 the successful evolution and retrieval of phages that, together, can infect all of the 31 resistant *E. coli*
214 C phenotypes.

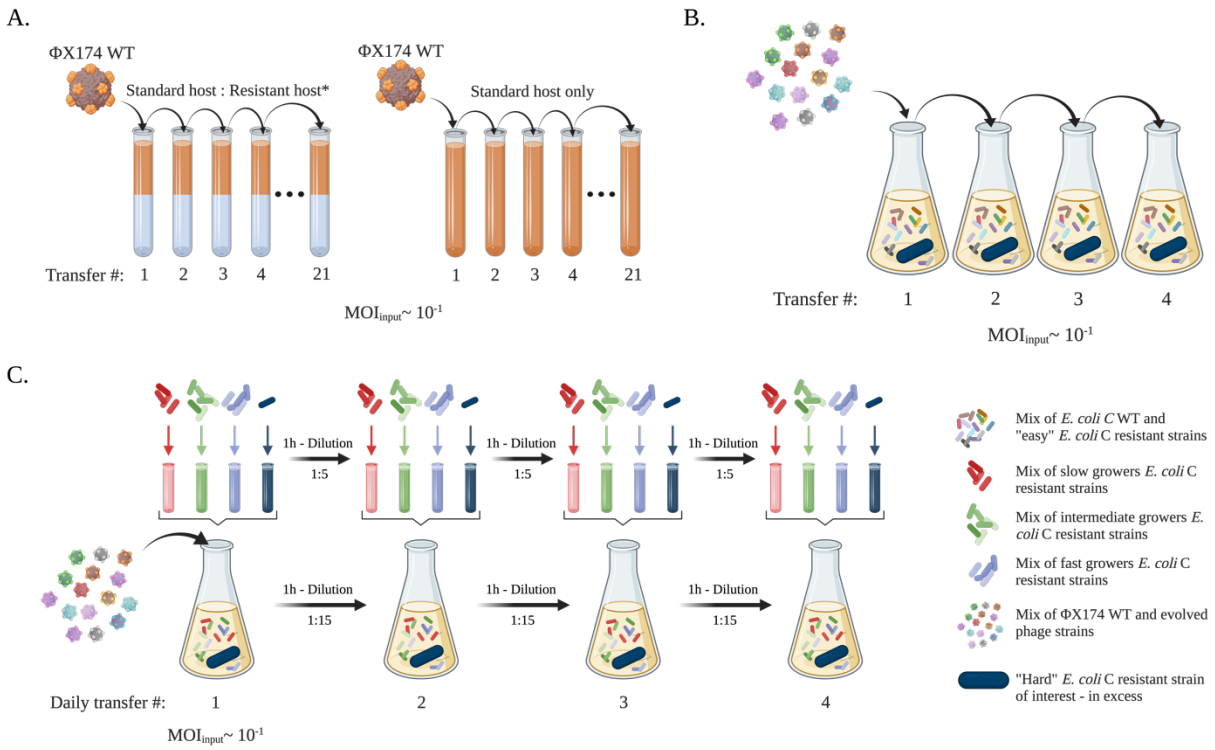

Fig. 3. Three phage evolution experiments used to overcome *E. coli* C resistance to wildtype ΦX174. A. First evolution experiment (standard): 31 independent lineages, each founded by ΦX174 wildtype, were serially transferred daily for up to 21 days (21 transfers). Phages were grown on non-evolving (i.e., freshly prepared at each transfer) host cultures containing a mixture of *E. coli* C wildtype and one of the 31 initially resistant strains (see **Table S1**). The presence of *E. coli* C wildtype was necessary to propagate ΦX174 and avoid its dilution from one transfer to another. Phages capable of infecting the initially resistant host strain were isolated from 12 lineages. Three control lineages were included, where ΦX174 was cultured on only *E. coli* C wildtype. **B.** Second evolution experiment (increased diversity). A cocktail of ΦX174 wildtype and 14 evolved ΦX174 strains was generated (panel A – the two evolved phages infecting R5 and R19 were part of the final cocktail but removed from the mutational analysis, see **Text S1**). The phage cocktail was transferred daily for up to four days, on non-evolving host cultures containing: (i) *E. coli* C wildtype, (ii) the 14 host strains for which resistance had been overcome (permissive hosts), and (iii) an excess of one of the still-resistant strain of interest (non-permissive host). Phages capable of infecting two resistant strains of interest (*galU* and *waaG* mutants) were isolated from two lines. **C.** Third evolution experiment (increased diversity

233 and generations). The same cocktail used for the second evolution experiment (panel B) was
234 transferred four times daily for four days (i.e., a maximum of 16 transfers) on non-evolving host
235 cultures containing: (i) *E. coli* C wildtype, (ii) the 14 strains for which resistance had been overcome
236 (permissive hosts), and (iii) one of the still-resistant strain of interest (non-permissive host). Notably,
237 all transfers completed on the same day involved transferring both phage and bacteria; supernatants
238 were collected on every fourth transfer, and only phages were transferred. Phages capable of infecting
239 two resistant strains of interest (*waaP*/*pssA* mutants) were isolated from two lines. Details of the
240 evolved phages are presented in **Table S2**, and further methodological details are provided in
241 **Methods**.
242
243 Increasing both phage and host diversities in the second and third evolution experiments accelerated
244 the adaptation of ΦX174 to resistant *E. coli* C strains. While our experiment quickly gave rise to phages
245 able to infect most non-permissive strains (**Fig. 4A**), some phage-resistant hosts could only be infected
246 when both host and phage diversities were increased (**Figs. 4B and 4C**).
247

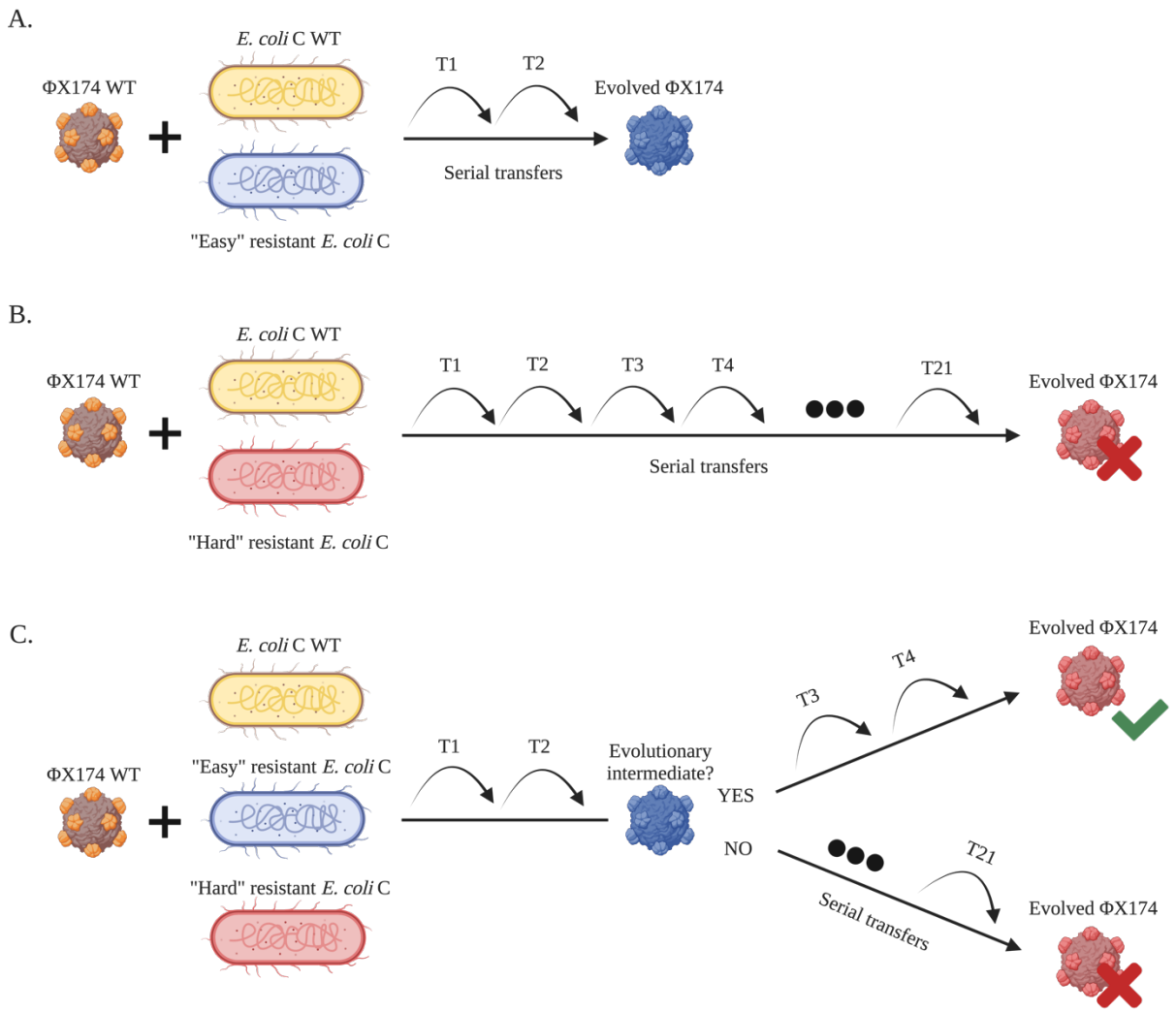

Fig. 4. Increased host diversity facilitates viral adaptation. A. ΦX174 wildtype evolves on *E. coli* C wildtype and an easy-resistant *E. coli* C strain. Adaptation to the resistant mutant is fast and only requires a few transfers. **B.** ΦX174 wildtype evolves on *E. coli* C wildtype and a hard-resistant *E. coli* C strain that it failed to infect within 21 standard serial transfers. Infecting this resistant strain may be difficult and take a long time. **C.** ΦX174 wildtype evolves in a three-host mix containing *E. coli* C wildtype and two *E. coli* C resistant strains: one easy and one hard. Phage adapts quickly to the easy-resistant phenotype. If the infection of the easy-resistant strain leads to the production of an evolutionary intermediate phage, then the hard phenotype can be infected after a few more transfers. If no evolutionary intermediate phage is produced, then no phage evolves to infect the hard-resistant *E. coli* C strain.

261 To identify the mutation(s) responsible for the re-infection of the resistant mutants, we performed
262 whole genome re-sequencing on the 16 evolved phages that successfully overcame the corresponding
263 resistance in one of the three evolution experiments (see **Methods**). We found mutations in *F* and/or
264 *H* genes in all 16 evolved phages (**Table S2**). Notably, all hard-resistant *E. coli* C strains - those whose
265 resistance was overcome in the second and/or third evolution experiments - are only infected by
266 phages carrying four mutations (see **Tables S1 and S2**).
267
268 The evolutionary emergence of a multi-mutation phage in a two-strain evolution experiment is
269 expected to require a large number of transfers (**Fig. 4B**). However, this process is significantly
270 accelerated by propagating a diverse mixture of phages. If some of the phages are evolutionary
271 intermediates (i.e., carry a subset of mutations required to overcome hard resistance) then the
272 mutations required to overcome hard resistance can emerge in a single mutational step, either by
273 recombination (Rokyta et al. 2006) or by adding mutation to an existing set (**Fig. 4C**). For example,
274 the hard-resistant strain *E. coli* C R22 (a *galU* mutant; see **Table S1**) is overcome in the second
275 evolution experiment by ΦX174 R22 T1, a phage that carries four mutations (three in *F*, one in *H*;
276 see **Table S2**). Each of these mutations was present in the phage cocktail used to initiate the
277 evolutionary lineage: ΦX174 R18 T4 and ΦX174 R8 T6 contain three of the four mutations, and the
278 final mutation is found in ΦX174 R10 T6. The evolved phage infecting R22 may, therefore, be the
279 product of a recombination event between ΦX174 R10 T6 and ΦX174 R18 T4 (or ΦX174 R8 T6).
280 Alternatively, ΦX174 R18 T4 or ΦX174 R8 T6 could have acquired a single additional mutation.
281 Thus, adaptation to certain easy-resistant LPS phenotypes yields evolutionary intermediate phages that
282 can recombine or acquire a few additional mutations to infect a hard-resistant LPS structure.
283
284 Our results show that high host diversity can facilitate the evolution of phages to infect resistant
285 strains. In contrast, Sant et al. showed that high host diversity hinders phage evolution (Sant et al.
286 2021). The major difference between the experiments is the difficulty of the evolutionary problem
287 posed. Sant et al. only evolved phages to infect easy-resistant strains, strains that could be infected by
288 phages after seven to eight transfers through the acquisition of a few mutations. Evolutionary
289 intermediates will not be required in this situation (**Fig. 4A**). However, as we show here, it is very
290 difficult to infect hard-resistant strains starting with low phage and host diversities (**Fig. 4B**). Hence,
291 increasing the host diversity will accelerate the evolution of phage adaptation under conditions where
292 the additional hosts allow the evolution of intermediate phage phenotypes (**Fig. 4C**).

293

294 **ΦX174 overcomes *E. coli* C resistance by mutations in the F capsid and H minor spike**
295 **proteins**

296 The 16 evolved phages collectively carry 40 mutations, 15 of which are unique (**Fig. 5A and Table**
297 **S2**). All are non-synonymous and occur in either *F* (encoding the viral capsid) or *H* (encoding the
298 minor spike protein involved in viral DNA injection) genes (**Figs. 5B and 5C**). The majority of phages
299 (13 of 16) carry between two and four mutations (**Fig. 5D**). These results are consistent with previous
300 studies demonstrating that mutations in *F* and *H* are relevant for the adaptation of ΦX174 to novel
301 hosts (Weisbeek et al. 1973; Crill et al. 2000; Cox and Putonti 2010).

302

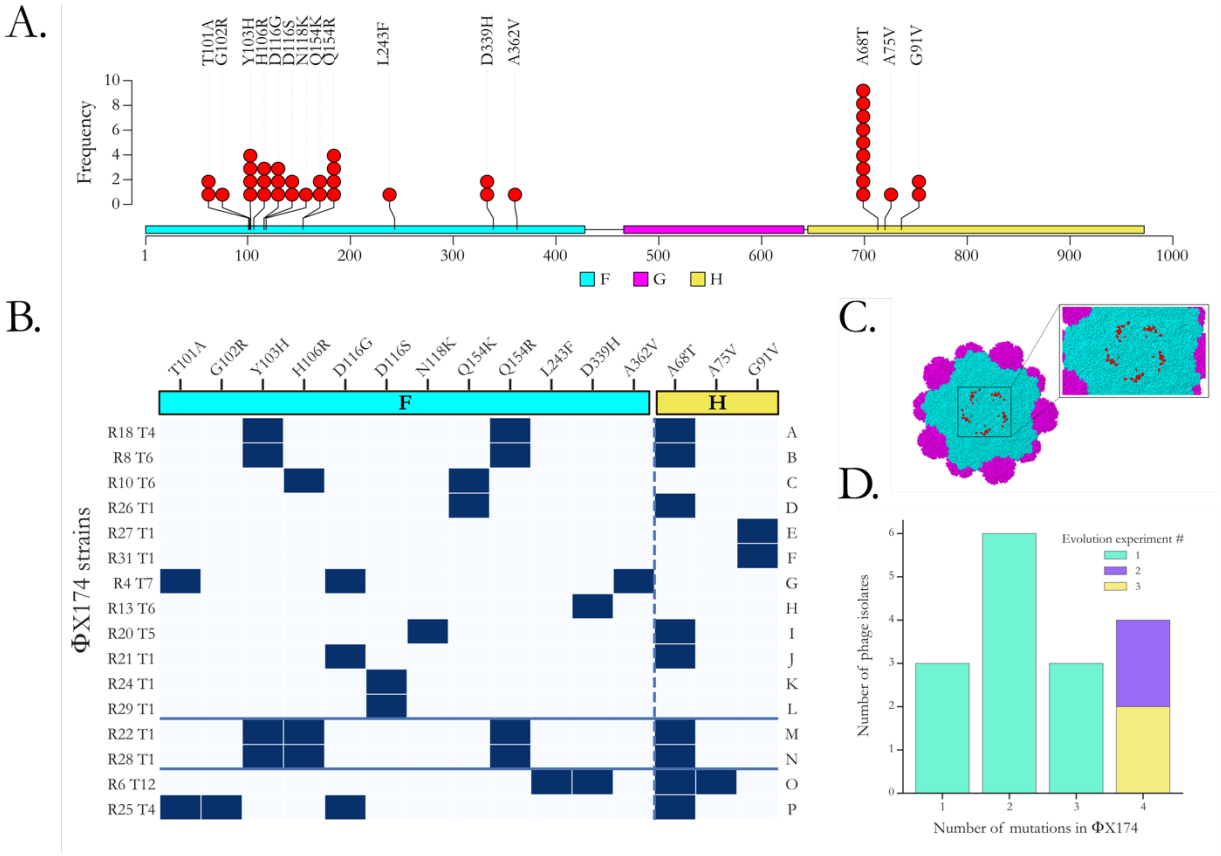

303

304

305 **Fig. 5. Adaptation of ΦX174 to resistant strains of *E. coli* C. A.** Positions of all predicted amino
306 acid changes in the F (viral capsid; coloured in cyan) and H (minor spike; coloured in yellow) proteins
307 observed in the 16 evolved ΦX174 strains. No mutation was found in the G protein (major spike;
308 coloured in magenta) despite being an integral part of ΦX174's recognition system and the first
309 contact point with the LPS structure (Kawaura et al. 2000; Sun et al. 2017). **B.** Substitution matrix of

310 all amino acid changes observed in ΦX174. ΦX174 strains are ordered based on the predicted LPS
311 structures they infected during the evolution experiments (A-F: overcame heptoseless *waaC* and *hldE*
312 mutants; G-L: overcame *waaO* mutants; M-N: overcame *galU* and *waaG* mutants; O: overcame
313 *waaP*/*pssA* mutant; P: overcame *rfaH* mutant). The solid blue lines separate the evolved phages
314 according to the evolution experiment from which they were isolated (A-L: first; M-N: second; O-P:
315 third). The x-axis shows amino acid substitutions in the F and H proteins (separated by the dashed
316 line), R# indicates the resistant bacterial strain the phage evolved on, and T# is the number of
317 transfers required to overcome host resistance. **C.** Location of protein changes on the ΦX174 three-
318 dimensional structure. The F capsid proteins are coloured in cyan, and the G major spike proteins are
319 in magenta. Residues affected by the mutations in this study are in red and shown for one F capsid
320 unit only. The G protein spike (above that pictured here) has been removed to improve visualisation.
321 The image was generated using Geneious Prime (version 2020.1.2) and Protein Data Bank accession
322 code 2BPA (McKenna et al. 1992). Changes in the H protein cannot be displayed as they all occur
323 outside of the currently determined crystallographic structure. **D.** Barplot of the number of evolved
324 phage isolates carrying 1, 2, 3, 4 mutations. Most phage isolates – particularly those isolated from the
325 second and third evolution experiments – carry multiple mutations.
326
327 Parallel evolution was common in our evolved phages, particularly in the control lines and the lineages
328 that failed to infect their corresponding resistant *E. coli* C strains during the first evolution experiment
329 (see **Table S3**). Of the three controls and 15 resistant lines that remained uninfected by their own
330 phage, a total of 33 mutations were detected, but only ten were unique. All these mutations are located
331 in the *F* gene, except one in the *A*/*A** genes. *A* gene is involved in the stage II and III of phage DNA
332 replication (Barrell et al. 1976; Sanger et al. 1978), while the *A** gene is a non-essential gene that may
333 play a role in the inhibition of host cell DNA replication and superinfection exclusion (Eisenberg and
334 Ascarelli 1981). The mutation in the *F* gene at genomic position 2280 (causing amino acid change
335 S427L in the F protein) arose in 13 lineages. Among them, nine (69 %) carry between one to three
336 additional mutations. High degrees of parallel evolution have also previously been observed in ΦX174
337 wildtype strains and other viruses (Bull et al. 1997; Wichman et al. 1999; Remold et al. 2008; Bertels
338 et al. 2019; Bertels et al. 2021) and is an indicator of either (i) a low number of mutational targets with
339 similar high fitness gains (many more targets with lower fitness may exist but these will not be
340 outcompeted by the high fitness mutants), or (ii) mutational bias towards certain positions in the

341 genome (Lind et al. 2019; Bertels et al. 2021). While these substitutions may not allow the infection of
342 resistant *E. coli* C strains, they are probably adaptations to our evolution experiment.
343
344 We also observed high levels of parallel evolution in the phage strains (isolates) that evolved to infect
345 *E. coli* C mutants with the same predicted LPS phenotype (**Figs. 5A and 5B**). Parallelism was especially
346 remarkable among phages infecting the four bacterial strains with the shortest (deep rough
347 heptoseless) predicted LPS structure (see **Fig. 2**). The four phages infecting *E. coli* C R18, R8, R10,
348 and R26 all carry an amino acid substitution at position 154 in the F protein (either Q154K or Q154R).
349 In addition, the two phage strains adapted to the *E. coli* C mutants R8 (*hldE* mutant) and R18 (*waaC*
350 mutant) also carry the mutations Y103H in the F protein and A68T in the H protein. Finally, while *E.*
351 *coli* C R27 and R31 both became resistant via the same amino acid substitution in HldE (G27A), their
352 corresponding phages evolved similarly by each acquiring a different mutation that led to the same
353 change at the protein level (G91V in the H protein).
354
355 Parallel evolution was also observed in phages infecting bacteria within several other classes of
356 predicted LPS structure. For example, the mutation at position 116 in the F protein (either D116G or
357 D116S) occurred in four different phages all infecting different *waaO* mutants (**Figs. 5A and 5B,**
358 **Table S2**). Parallel evolution in phages that evolved to infect *E. coli* C strains with the same predicted
359 LPS structure generally supports the predicted classes of LPS structure. However, analyses in the
360 following section demonstrate that LPS structure predictions generally underestimate LPS diversity.
361
362 **Evolved phages can be used to discriminate between LPS phenotypes**
363 To determine precisely which of the 16 evolved phages can infect which of the 31 initially resistant *E.*
364 *coli* C strains each (i.e., the infection pattern of each phage), a cross-infection assay was performed
365 (**Fig. S3**). This involved measuring the infectivity of all possible host-phage combinations by two
366 distinct methods: (i) phage spotting on host lawns and (ii) host spotting on phage lawns. In cases
367 where a mismatch between the two results was observed, standard plaque assays were additionally
368 applied (see **Methods**).
369
370 If our predictions – based on the current understanding in the literature – of seven distinct LPS
371 structures among the 31 initially resistant *E. coli* C strains are accurate (see **Fig. 2 and Table S1**), then
372 all phages that evolved to infect a mutant with a given predicted LPS structure are expected to cross-

373 infect all other host strains with the same predicted LPS structure. That is, the infection patterns in
374 **Fig. S3** would be identical for each class (colour) of *E. coli* C mutant.
375
376 To visually determine whether infection patterns cluster according to the predicted LPS structures, a
377 hierarchical agglomerative clustering analysis was performed on the infection matrix in **Fig. S3**. Of
378 the six predicted LPS structures that occur in at least two *E. coli* C mutants, three form unbroken
379 clusters with respect to infectivity patterns (cyan, light purple, and dark purple highlighting in **Fig. 6**)
380 and three do not (magenta, yellow, green highlighting). Each group is discussed in more detail below.
381

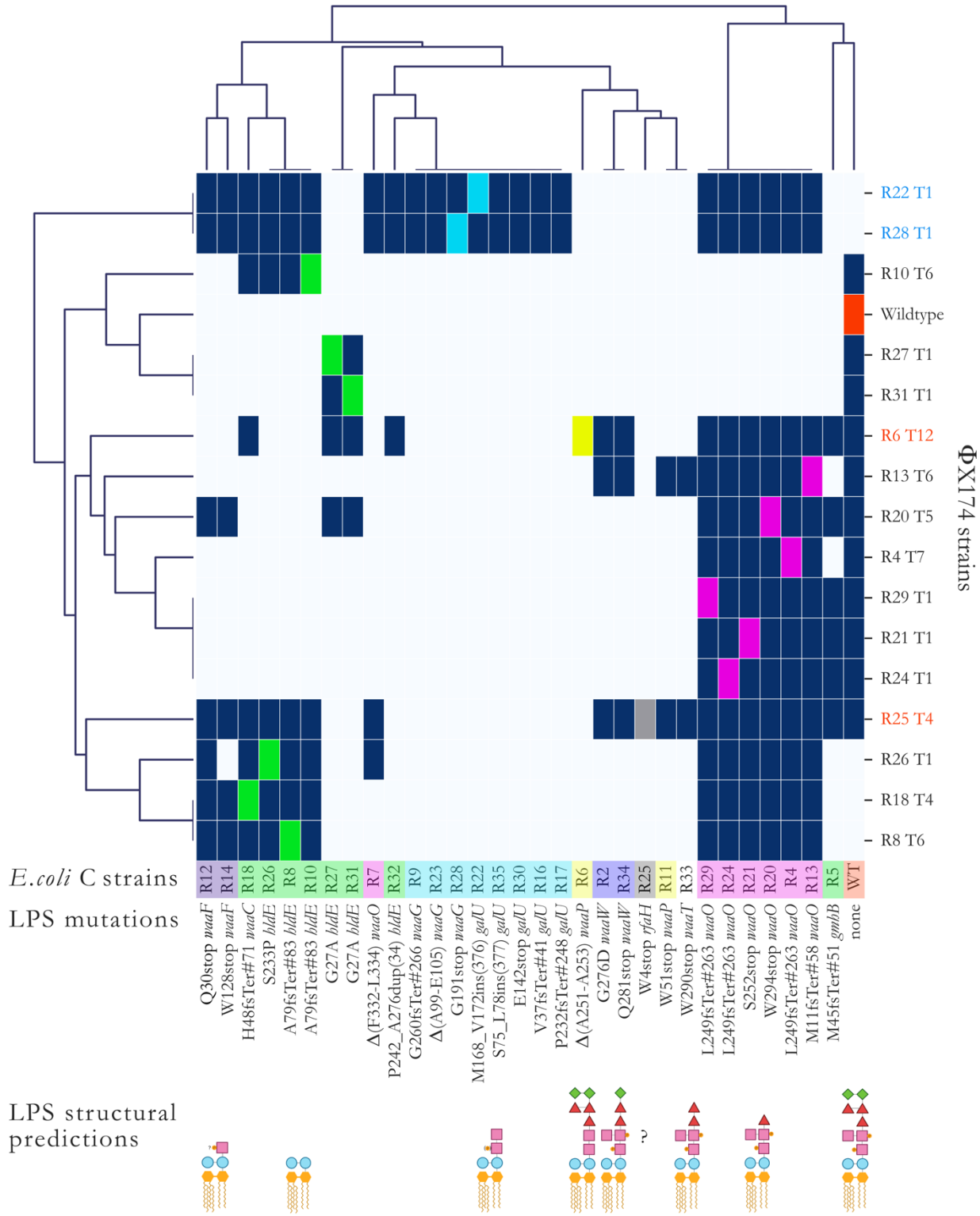

Fig. 6. Hierarchical agglomerative clustering analysis of the host ranges of evolved phage. To unravel structures in the heatmap infection matrix (see **Fig. S3**), we performed a clustering analysis

386 using the default settings of the Seaborn library (version 0.11.2) for Python (version 3.7.4). Briefly,
387 each data point corresponds to either presence (dark blue) or absence (light blue) of phage infections
388 determined from the combination of the different spotting test assays' results (**Methods**). The linkage
389 method computes the distance between them, then repeatedly combines the two nearest clusters into
390 larger clusters until a single cluster is left. *E. coli* C strains are coloured based on their predicted core
391 LPS structure (see **Fig. 2**). Phage names in black were obtained during the first 21 serial transfers (first
392 evolution experiment). Phage strains in blue were obtained in the second evolution experiment (phage
393 cocktail, one transfer per day). Phage strains in red were obtained in the third evolution experiment
394 (phage cocktail, four transfers per day). Dark blue squares=infection, light blue square=no infection,
395 coloured square=control infection by a phage evolved on that host. R# indicates the number of the
396 resistant strain the phage evolved on, and T# is the transfer number where plaques were first observed.
397 "?": core LPS structure of *E. coli* C R25 (*rfaH* mutant) could not be predicted. "INS": insertion.
398 "DUP": duplication. "stop": stop codon. "Δ": deletion. Examples: L249fsTer#263 indicates a
399 frameshift (fs) leading to a premature codon stop (Ter); the position of the premature stop codon is
400 in parentheses. S75_L78ins(377) indicates an insertion; the two flanking amino acids are separated by
401 a "_" and followed by the number of inserted amino acids in parentheses. Δ(A99-E105) indicated
402 deletion; two flanking amino acids are separated by a "-". P242_A276dup(34) indicates a duplication;
403 the two flanking amino acids are separated by a "_" and followed by the number of duplicated amino
404 acids in parentheses.
405
406 *LPS predictions that cluster by infection pattern.* The identical ΦX174 mutants R22 T1 and R28 T1 that
407 evolved to infect resistant strains with mutations in *galU* (*E. coli* C R22) and *waaG* (*E. coli* C R28) can
408 cross-infect all eight *E. coli* C mutants predicted to exhibit the same LPS structure (*E. coli* C R9, R16,
409 R17, R22, R23, R28, R30, R35; highlighted in cyan in **Figs. 6 and S3**). Furthermore, both *E. coli* C
410 *waaW* mutants (R2 and R34; light purple) are cross-infected by the same three evolved phage
411 genotypes (R6 T12, R13 T6, R25 T4). Also, both *E. coli* C *waaF* mutants (R12 and R14; dark purple)
412 are infected by a near-identical set of seven (R12) or six (R14) phages. In each of these cases, phage
413 infectivity patterns appear to be a good indicator of host LPS phenotype.
414
415 *LPS predictions that do not cluster by infection pattern.* Six of the seven *E. coli* C *waaO* mutants (highlighted
416 in magenta in **Figs. 6 and S3**) can be cross-infected by the same set of 13 phages. The seventh *waaO*
417 mutant (*E. coli* C R7) was the only *waaO* mutant for which the corresponding phage lineage did not

418 evolve to infect the resistant mutant in the first evolution experiment. It can only be infected by the
419 phage infecting R26 and phages that evolved in the second and third evolution experiments (**Fig. 6**).
420 Hence, it is likely that the LPS structure of R7 differs from that of the other *waaO* mutants. The
421 difference could conceivably result from residual (or altered) WaaO function; *E. coli* C R7 carries an
422 in-frame deletion of a 6-bp repeat in *waaO*, which alters two WaaO residues but leaves the remainder
423 of the protein intact (see **Table S1**). Because R7 is close to the *galU*/*waaG* mutants (**Figs. 6**), it may
424 be possible that its LPS structure resembles the ones of the *galU*/*waaG* mutants. However, more
425 detailed LPS studies are needed to elucidate the LPS structure of R7.
426
427 The infection patterns of the two *waaP* mutants *E. coli* C R6 and R11 (highlighted in yellow in **Figs. 6**
428 **and S3**) also suggest that, in contrast to the prediction, these strains possess different LPS structures.
429 R6 is infected by a single phage that evolved directly on host R6 (phage R6 T12 from the third
430 evolution experiment), while R11 is cross-infected by two different phages (phage R13 T6 from the
431 first evolution experiment and phage R25 T4 from the third evolution experiment). *E. coli* C R6 was
432 the last resistant strain to be infected by an evolved phage, and the evolved phage infecting R6 cannot
433 cross-infect R11.
434
435 The R11 mutation introduces a premature codon stop at the beginning of the *waaP* gene (**Fig. 6 and**
436 **Table S1**). *WaaP* is special because it is not required for completing the backbone structure of the
437 LPS (Yethon et al. 1998). The deletion of this gene should, therefore, lead to a unique LPS structure
438 (see **Fig. 2**). Instead, the cluster map analysis indicates that R11 displays an LPS phenotype comparable
439 to the rough LPS phenotype of R33, a *waaT* mutant (**Fig. 6**). These similarities may be caused by a
440 polar effect of the R11 mutation in *waaP* on *waaT* downstream. This effect may have resulted in a
441 decrease or an alteration of *waaT* activity leading to a truncation of the outer core LPS similar to the
442 one in R33.
443
444 The combination of phages that can infect each of the eight heptoseless *E. coli* C mutants predicted
445 to have the shortest LPS structure (**Fig. 2**; green highlighting in **Figs. 6 and S3**) is remarkably
446 different. These *E. coli* C strains cluster into four different phenotypic sub-groups (**Fig. 6**). The first
447 sub-group consists of *E. coli* C R8, R10, R18, and R26. Each of these strains can be cross-infected by
448 their corresponding evolved phages, regardless of their genotypes (a mixture of *waaC* or *hldE* mutants).
449 However, none of the four evolved phages can cross-infect *E. coli* C R27 or R31 (*hldE* mutants). *E.*

450 *coli* C R27 and R31 comprise the second sub-group. Both *E. coli* C R27 and R31 and their
451 corresponding evolved phages acquired identical genotypes and, not surprisingly, they also share
452 phenotypes. *E. coli* C R5 (*gmhB* mutant) and *E. coli* C R32 (*hldE* mutant) fall into a third and a fourth
453 sub-groups. *E. coli* C R32 is the only heptoseless mutant for which the corresponding phage lineage
454 failed to infect during the first evolution experiment. Only a very narrow but different set of evolved
455 phages can infect R5 and R32 (**Figs. 6 and S3**).
456
457 A total loss of function in *hldE* or *waaC* genes always leads to a complete truncation of the inner core
458 LPS (**Fig. S2A**). Thus, the involvement of these two genes in the production of the deep rough
459 phenotypes (highlighted in green in **Figs. 6 and S3**) cannot explain the vast phenotypic diversity in
460 LPS structures. For example, *E. coli* C R8, R10, R18, and R26 belong to the same phenotypic group
461 despite having both *hldE* or *waaC* mutated, while R27, R31, and R32 (all *hldE* mutants) do not belong
462 to this group (**Fig. 6 and Table S1**). Instead, the location and type of mutation are more likely to
463 cause the observed LPS structure diversity.
464
465 Interestingly, HldE is a bifunctional protein, where each function is performed by a different domain:
466 HldE1 (from M1 to T318) and HldE2 (from M344 to G477) (Valvano et al. 2000; Kneidinger et al.
467 2002; Raetz and Whitfield 2002; McArthur et al. 2005). Each domain has the potential to affect the
468 LPS structure, but all four unique *hldE* mutations occur within the first domain only, resulting in at
469 least three different LPS phenotypes (**Fig. 6 and Table S1**). These LPS phenotypes are caused by
470 three different types of mutations (duplication, missense mutations, and frameshift) in different parts
471 of the same domain. Yet, there is no obvious correlation between the LPS phenotypes and mutation
472 positions and/or types. The phenotypic diversity produced by these mutations in a single domain of
473 a single gene is surprising and highlights our extremely limited understanding of LPS biology.
474
475 The mutated *gmhB* gene in *E. coli* C R5 is involved in the production of yet another deep rough
476 phenotype. Previous research demonstrated that the deletion of *gmhB* only causes a partial defect in
477 the synthesis of the LPS core, resulting in the formation and co-existing of a heptoseless and a heptose-
478 rich form of LPS molecules (Kneidinger et al. 2002). The *gmhB* mutation in R5 is an early frameshift
479 leading to a premature stop codon. Hence, we assume that the effect is similar to what was found by
480 Kneidinger et al., a mix of deep rough and wildtype LPS molecules on the outer bacterial cell

481 membrane. This hypothesis is supported by the fact that R5 most closely clusters with the wildtype in
482 our infection matrix.
483
484 **Linking phage genotype to phenotype**
485 Phage infectivity patterns (host ranges) can be used to construct phage genotype-phenotype maps.
486 For example, every phage strain that loses the ability to infect *E. coli* C wildtype has a combination of
487 two mutations: A68T in the H protein and Q154K/R in the F protein (**Figs. 5B and 6**). In isolation,
488 A68T confers the ability to infect *waaO* mutants and Q154K/R to infect [R8, R18, R10, R26]-
489 heptoseless mutants. The two mutations combined allow the phage to infect both heptoseless and
490 *waaO* mutants, but cannot infect the *E. coli* C wildtype (**Figs. 5B and 6**). ΦX174 R25 T4 is the only
491 phage that can infect all three genotypes: *waaO*, the [R8, R18, R10, R26]-heptoseless mutants, and *E.*
492 *coli* C wildtype. Presumably, because this phage does not contain the Q154K/R mutation and instead
493 uses another set of mutations that allows R25 to infect [R8, R18, R10, R26]-heptoseless mutants
494 (**Table S2**).
495
496 ## Discussion
497 Our experiments have shown that *E. coli* C can become resistant to ΦX174 infection through
498 mutations in genes involved in the LPS biosynthesis or assembly. ΦX174 can, in turn, evolve to
499 reinfect initially resistant *E. coli* C strains by acquiring mutations in genes involved in host recognition
500 or DNA injection. Similar to ΦX174 wildtype, the evolved phages are highly host-specific and hence
501 can be used to distinguish between bacteria with different LPS structures. Such high host specificity
502 allows testing of the currently accepted LPS structure model, where LPS structures are determined by
503 the presence and absence of LPS synthesis and assembly genes. Our data on phage infectivity show
504 that LPS diversity is far greater than the current model suggests. Presumably, the modulation of LPS
505 gene activity leads to a variety of LPS phenotypes. Our findings can potentially be applied to other
506 phages that use LPS as a single or complementary receptor for host infection (Bertozzi Silva et al.
507 2016; Latino et al. 2016; Broeker and Barbirz 2017). The LPS is a major structural component of the
508 outer membrane of Gram-negative bacteria (Zhang et al. 2013), and its biosynthesis and assembly are
509 conserved among bacterial species.
510
511 Another major finding of our study is that increasing phage and host diversity allows the infection of
512 hard-resistant phenotypes (see **Fig. 4C**). This phenomenon – the successful infection of hard-resistant

513 phenotypes – is similar to a receptor shift observed with phage λ (Meyer et al. 2012). Phage λ also
514 requires at least four mutations to infect the novel OmpF receptor in *E. coli* B, making it almost
515 impossible to evolve from the wildtype phage in a single step (Burmeister et al. 2016). Evolving all
516 four mutations in one λ phage genome first required the presence of λ phage evolutionary
517 intermediates that already carried specific mutations. These evolutionary intermediates may have
518 arisen from the infection of easy-resistant *E. coli* B mutants (*malT* loss-of-function mutants) that could
519 still spontaneously induce low levels of the traditional host receptor, LamB. By increasing the host
520 diversity, phage λ eventually acquired additional mutations (four in total) to overcome the hard-
521 resistant *E. coli B* mutants (*lamB* loss-of-function mutants) (Meyer et al. 2012; Gupta et al. 2022).
522 Similarly, we showed that the successful infection of *waaG*, *galU*, *rfaH*, and *waaP*/*pssA* resistant strains
523 became accessible by increasing host and phage diversity.
524
525 Our experiments suggest that it may be possible to breed well-established model phages such as
526 ΦX174 to infect a wide range of currently resistant pathogenic *E. coli* strains. If possible, then this
527 could make ΦX174 a promising therapeutic agent. Currently, instead of breeding well-known model
528 systems to infect pathogenic bacteria, unknown phages that can infect specific bacterial pathogens are
529 isolated from environmental samples (Chan et al. 2018). These unknown phages, however, still have
530 to be characterized. Their safety has to be ensured by a process that, in the end, may drastically be
531 more time-consuming than breeding well-studied model systems. Safety concerns regarding novel
532 phages are significant due to their potential to carry dangerous toxins and antibiotic-resistance genes
533 (Krüger and Lucchesi 2015; Colavecchio et al. 2017; Jamet et al. 2017). The considerable knowledge
534 acquired from decades of research on ΦX174 structure, life cycle, and evolution showed that ΦX174
535 does not carry virulence genes. ΦX174 is also highly host-specific (Michel et al. 2010), meaning that
536 it will be harmless to the patient's microbiota, in contrast to phages with broader infectivity or
537 antibiotics known to disrupt the microbiota and lead to adverse health outcomes (Ramirez et al. 2020).
538 Furthermore, its use as a marker of immune responses in patients has already been approved *in vivo*
539 by the FDA in specific case studies (Rubinstein et al. 2000; Bearden et al. 2005). ΦX174 can easily be
540 manipulated in a laboratory unlocking its potential as a powerful therapeutic agent. For all these
541 reasons, we believe that bacteriophage ΦX174 could become a promising therapeutic agent.
542
543

544 ## Methods

545

546 **Bacterial and phage strains.** The ancestral *Escherichia coli* strain C used in this study differs from the
547 one uploaded on the NCBI website (GenBank accession number CP020543.1) by the presence of 9
548 additional insertions and two nucleotide substitutions (c → t at the position 1,1720,214 and g → t at
549 the position 1,190,560). The genomic sequence of CP020543.1 was manually modified using Geneious
550 Prime (version 2020.1.2). All resistant bacterial strains generated in this study are derived from our
551 ancestral *E. coli* C strain. All bacteriophage strains are derived from the ancestral coliphage ΦX174
552 (GenBank accession number AF176034). AF176034 genomic sequence was downloaded from the
553 NCBI website and manually annotated using Geneious Prime (version 2020.1.2). Whole-genome re-
554 sequencing on ΦX174 wildtype's glycerol stock showed no difference to the NCBI sequence.
555 Complete genomes of *E. coli* C WT and ΦX174 WT used as references have been deposited in Zenodo
556 (doi: 10.5281/zenodo.6952399). The *E. coli* C and ΦX174 ancestral strains were provided by Holly A.
557 Wichman (Department of Biological Sciences, University of Idaho).

558

559 **Media and growth conditions.** Phage and bacteria were grown in a shaking incubator (New
560 Brunswick™ Innova® 44) at 37°C, 250 rpm, in LB (Lysogeny Broth, Miller) medium supplemented
561 with $CaCl_2$ and $MgCl_2$ at a final concentration of 5 mM and 10 mM, respectively. Solid LB agar (1.5 %
562 agar) was used to plate both bacteria and phages. When plating phage, top agar overlay (0.5 % agar),
563 also called semi-solid agar (SSA) in this study, was supplemented with $CaCl_2$ and $MgCl_2$ at a final
564 concentration of 5 mM and 10 mM respectively. PBJ solution (Phage Buffer Juice: 2.03 % Tris-HCl,
565 0.61 % $MgCl_2.6H_2O$) was used for serial dilutions. *E. coli* colony plates were generated by streaking
566 with a sterile loop a scrap of the corresponding bacterial glycerol stock on the surface of a solid LB
567 plate and incubated inverted overnight. After incubation, the colony plates were stored at 4°C for a
568 maximum of two weeks. Overnight bacterial liquid cultures were systematically started by inoculating
569 a single colony in 5 ml of LB supplemented with $CaCl_2$ and $MgCl_2$ at a final concentration of 5 and 10
570 mM, respectively, shaken at 250 rpm. Phage infections were either started from (i) a scrap of the
571 corresponding phage glycerol stock resuspended in 100 µl of PBJ or (ii) a single plaque isolated from
572 the top agar overlay with a sterile cut tip (a circle of agar) directly inoculated inside the bacterial culture.
573 Overnight incubations of both plates and cultures were set up for ~16-17 hours at 37°C.

574

575 **Measuring the growth of each resistant *E. coli* C strain**

576 To assess the impact of LPS modifications harboured by the different *E. coli* C resistant mutants on
577 their growth, two independent cultures of each resistant strain were grown at 37°C, 250 rpm for 17
578 hours. 180 μl of each overnight culture was inoculated into a 14 ml sterile tube (FALCON®)
579 containing 5 ml of LB (supplemented with $CaCl_2$ and $MgCl_2$ at final concentrations of 5 and 10 mM,
580 respectively) pre-warmed at 37°C. Incubation time was set to six hours at 37°C, 250 rpm. Optical
581 density at 600 nm (OD600) was measured every 30 minutes with an Ultrospec 10 (Biochrom®). *E.*
582 *coli* C wildtype was used as a reference. The mean OD600 values at each time point for each bacterial
583 mutant were calculated and plotted.
584
585 **Isolation and storage of *E. coli* C strains with resistance to wildtype ΦX174.** To avoid
586 competition and to produce a diverse set of phage-resistant bacterial mutants with different growth
587 phenotypes, we generated ΦX174-resistant *E. coli* C strains on agar plates. Thirty-five *E. coli* C wildtype
588 colonies were randomly chosen from an agar plate, and each was used to inoculate an independent
589 overnight liquid culture. 50 μl of each stationary phase culture was mixed with 50 μl of a high titer
590 (~10^9 plaque-forming unit pfu ml^{-1}) stock of ΦX174 wildtype lysate, immediately plated with sterile
591 beads on LB plates, and incubated at 37°C overnight. From each plate, half a randomly chosen colony
592 was used to inoculate a fresh overnight LB liquid culture. Once grown, a sample from each culture
593 was mixed with glycerol saline solution and frozen at -80°C (giving strains *E. coli* C R1-R35). To
594 confirm the resistance to wildtype ΦX174, the remaining half of each colony was streaked onto an
595 LB plate soaked with 100 μl of the high titer ΦX174 wildtype lysate and incubated at 37°C overnight.
596
597 **Phage lysate preparation.** To extract phages in infected host cultures, ten to twelve drops of
598 chloroform were added to growing *E. coli* C-phage co-cultures and vortexed for at least 30 seconds to
599 kill the bacteria. Cultures were then centrifugated at 5000 rpm for 10 min at 4°C. Supernatants (phage
600 lysates) were transferred to sterile 5 ml Eppendorf tubes and stored at 4°C. 1 ml of each lysate was
601 stored with glycerol saline solution and frozen at -80°C.
602
603 **First phage evolution experiment - Standard**. The protocol from Bono *et al.* (Bono et al. 2012) was
604 adapted to evolve phages that can infect resistant *E. coli* C strains. Of R1-R35 – the 35 *E. coli* C strains
605 resistant to ΦX174 wildtype, see above – 31 were used for the first phage evolution experiment
606 (excluding R1, R3, R15, and R19; see **Results** and **Text S1**). Thirty-one ΦX174 lineages were each

607 founded by ΦX174 wildtype and serially transferred daily, up to 21 days (21 transfers) in cultures
608 containing a mix of *E. coli* C wildtype (permissive strain) and one resistant *E. coli* C strain (non-
609 permissive strain; R2-R35). For each transfer, permissive and non-permissive bacteria were grown
610 separately until they reached the log phase, then mixed in at a specific ratio depending on the growth
611 of the non-permissive strain (see **Figs. 3A and S4** and **Supplementary Methods**) to a final volume
612 of 5 ml. At each transfer, freshly prepared susceptible cells were infected by ΦX174 at MOI_{input} ~0.1.
613 Infected cultures were shaken at 250 rpm, 37°C, for three hours. Phage lysates were isolated as
614 described in **Phage lysate preparation**. Phage lysates from the previous day were used to inoculate
615 the fresh bacterial mixes the next day. Transfers continued until phages were found to infect their
616 corresponding resistant *E. coli* C strain or until 21 transfers were reached. Three control lines were
617 also run in parallel by transferring ΦX174 at MOI_{input} ~0.1 in a culture containing *E. coli* C wildtype
618 only. See **Supplementary Methods** for a detailed version of the protocol.
619
620 **Second phage evolution experiment – Increased diversity.** A phage cocktail made of (i) the
621 wildtype ΦX174 and (ii) all ΦX174 strains that successfully re-infected their corresponding resistant
622 strains during the first phage evolution experiment was generated by first diluting each phage lysate
623 and mixing them at a roughly equal number of plaque-forming units (PFU). Fourteen phage strains
624 were used: ΦX174 R4 T7, ΦX174 R5 T2, ΦX174 R8 T6, ΦX174 R10 T6, ΦX174 R13 T6, ΦX174
625 R18 T4, ΦX174 R19 T1, ΦX174 R20 T5, ΦX174 R21 T1, ΦX174 R24 T1, ΦX174 R26 T1, ΦX174
626 R27 T1, ΦX174 R29 T1, and ΦX174 R31 T1. Phages infecting R5 and R19 were used for the cocktail
627 but removed from the mutational analysis (see **Text S1 and Table S4**). The phage cocktail was grown
628 and transferred daily for up to four days, on non-evolving host cultures containing (i) *E. coli* C wildtype,
629 (ii) the 14 host strains (see **Text S1** and **Table S4**) for which resistance had been overcome (permissive
630 hosts), and (iii) an excess of one of the still-resistant strain of interest (non-permissive host). For the
631 non-permissive host, we used R6 (*waaP*/*pssA* mutant), R22 (*galU* mutant), R25 (*rfaH* mutant), or R28
632 (*waaG* mutant; see **Table S1**). *E. coli* C R22 and R28 were chosen as representatives of the *galU* and
633 *waaG* mutants, respectively. Each bacterial strain (permissive and non-permissive) was grown
634 separately in LB liquid culture for one hour (37°C, 250 rpm), then pooled at a roughly equal number
635 of colony-forming units The resistant strain of interest was added in excess to give a final volume of
636 4 ml. Infected cultures were initiated by adding the phage cocktail (MOI_{input} ~0.1), shaken at 250 rpm,
637 37°C, for 5 hours (see **Fig. 3B**). Phage lysates were isolated as described in **Phage lysate preparation**.
638 Phage lysates from the previous day were used to inoculate the fresh bacterial mixes the next day. This

639 process was repeated until phages were found to infect their corresponding resistant *E. coli* C strains
640 or until four transfers had been completed. See **Supplementary Methods** for a detailed version of
641 the protocol.
642
643 **Third evolution experiment – Increased diversity and generations.** Protocol from the second
644 evolution experiment was adjusted to reduce the amount of time necessary to retrieve the desired
645 phages. The same phage cocktail used in the second phage evolution was grown and transferred daily,
646 four times a day, for up to four days on non-evolving host cultures containing (i) *E. coli* C wildtype,
647 (ii) the 14 host strains for which resistance had been overcome (permissive hosts), and (iii) one of the
648 still-resistant strain of interest (non-permissive host). We increased the number of serial transfers per
649 day from one to four, for a total of four days (16 transfers). *E. coli* C R6 (*waaP/pssA* mutant) and R25
650 (*rfaH* mutant, see **Table S1**) were used as non-permissive hosts. After reaching their exponential log
651 phase, bacterial strains (except the non-permissive hosts) were mixed depending on their growth
652 (**Figs. 3C and S4**, **Supplementary Methods**). New host cultures were kept in exponential growth
653 phase independently by transferring every hour 1:5 of the volume (1 ml) in fresh LB pre-heated at
654 37˚C (see **Fig. 3C**). Before each transfer, all host cultures were mixed together. Infected cultures were
655 started by adding the phage cocktail to the final host mix at MOI_{input} ~0.1, shaken at 250 rpm, 37˚C,
656 for one hour. After that, 1:15 of the volume of each infected culture was transferred in freshly mixed
657 bacterial cultures and infection continued for one hour (see **Fig. 3C**). This step was repeated for a
658 total of four transfers. The final (fourth) transfer lasted for two hours. All transfers completed on the
659 same day involved transferring both phage and bacteria; on every fourth transfer, supernatants were
660 collected and only phages were transferred. Phage lysates were isolated as described in **Phage lysate**
661 **preparation**. Phage lysates from the previous day were used to inoculate the first fresh bacterial mixes
662 the next day. This process was repeated until phages were found to infect their corresponding resistant
663 *E. coli* C strains or until four transfers had been completed. See **Supplementary Methods** for a
664 detailed version of the protocol.
665
666 **Isolation of evolved ΦX174 strains from evolution experiments.** To isolate pure, single clones
667 from the different evolution experiments, top agar overlays were prepared by mixing 100 μl of
668 undiluted phage lysates with 200 μl of an overnight culture of the corresponding resistant *E. coli* C
669 strain in 4 ml SSA. Plates were incubated inverted at 37˚C for ~16-17 hours. An isolated plaque was
670 chosen randomly for each phage lysate to infect cultures of the corresponding resistant *E. coli* C strains

671 (in exponential growth state) incubated at 37°C, 250 rpm, for 5 hours. Phage lysates were isolated as
672 described in **Phage lysate preparation**. Phage isolates were re-isolated from single plaques a second
673 time from their glycerol stocks. See **Supplementary Methods** for a detailed version of the protocol.
674

675 **Determination of the evolved phages' host range by spotting assays**

676 *Method 1.* Each top agar overlay was prepared by mixing 200 µl of an *E. coli* C strain from stationary
677 phase culture in 4 ml SSA, then poured on LB plates and dried for at least 15 minutes. Then, 3 µl of
678 each undiluted evolved phage lysate (between 10^7 and 10^9 pfu ml^{-1}) was dropped at the surface. *Method*
679 *2.* Each top agar overlay was prepared by mixing a volume of each phage lysate in 4 ml SSA at a final
680 concentration of ~10^7 pfu ml^{-1}, then poured on LB plates and dried for at least 15 minutes. Then, 3
681 µl of both undiluted and ten-fold diluted of each *E. coli* C strain (from overnight culture) were dropped
682 onto the surface with a pipette. For both methods, spots were dried for at least 30 minutes, and plates
683 were incubated inverted at 37°C for ~17 hours. *E. coli* C wildtype was used as a positive control
684 (permissive strain), and *E. coli* K-12 MG1655 as a negative control (non-permissive strain). A bacterial
685 host strain was classified as sensitive only when signs of lysis were detected using both methods in at
686 least two (of three) replicates per method. A phage-bacterium combination that yielded different
687 results between the two methods was tested in standard plaque assays. Finally, the host strain was
688 classified as sensitive if plaques were observed at both dilutions. See **Supplementary Methods** for a
689 detailed version of the protocol.
690

691 **Data visualisation.** The hierarchical agglomerative clustering analysis (Clustermap **Fig. 6**), the
692 heatmap (**Fig. S3**), and the growth curves (**Fig. S4**) were generated using the default settings of the
693 Seaborn library (version 0.11.2) for Python (version 3.7.4). All schematic drawings (**Figs. 1-4**, **S1 and**
694 **S2**) were created with BioRender.com. The Lollipop plot (**Fig. 5A**) was generated using trackViewer
695 Vignette: lollipopPlot (Lolliplot) in R (version 1.27.11).
696

697 **Whole genome re-sequencing.**

698 *Bacteria.* Samples were prepared for whole genome re-sequencing from 1 ml of stationary-phase
699 culture. Genomic DNA was extracted using the Wizard® Genomic DNA purification Kit (Promega,
700 Germany). Extracted DNA was tested for quality, pooled, and sequenced by the Max-Planck Institute

701 for Evolutionary Biology (Plön, Germany) using an Illumina Nextera DNA Flex Library Prep Kit to
702 produce 150 bp paired-end reads (Picelli et al. 2014).
703
704 *Phage*. ΦX174 samples were prepared for whole genome re-sequencing from 1 ml of phage lysate.
705 Genomic DNA was extracted using the QIAprep Spin Miniprep Kit (QIAGEN), then amplified by
706 performing 20 cycles of PCR using Q5® High-Fidelity 2X Master Mix (NEB) (final concentration
707 between 30-100 $ng.\mu l^{-1}$). The primers used for the amplification of the ΦX174 genome are listed in
708 **Table S6**. All PCR products were cleaned using the QIAquick PCR Purification Kit® (QIAGEN).
709 DNA samples were tested for quality, pooled, and sequenced by the Max-Planck Institute for
710 Evolutionary Biology (Plön, Germany). Sequencing was performed using an Illumina MiSeq DNA
711 Flex Library Prep Kit to produce 150 bp paired-end reads (Picelli et al. 2014).
712
713 The quality of the sequencing output from bacteria and phages was controlled using *FastQC* version
714 0.11.8. Reads were trimmed using *Trimmomatic*, assembled and analysed using the *breseq* pipeline version
715 0.33.2 (Barrick et al. 2014; Deatherage and Barrick 2014; Deatherage et al. 2015) and Geneious Prime
716 (version 2020.1.2).
717
718 **Sanger sequencing of ΦX174 *F* and *H* genes.**
719 Genomic DNA was extracted using the QIAprep Spin Miniprep Kit® (QIAGEN) (final
720 concentration between 30-100 $ng.\mu l^{-1}$). ΦX174's *F* and *H* genes were amplified by performing 35
721 cycles of PCR using Phusion® High-Fidelity PCR Master Mix with HF Buffer (ThermoFisher).
722 Primers used for this purpose are listed in **Table S6**. All PCR products were cleaned using the
723 QIAquick PCR Purification Kit®. Sanger sequencing was performed using the sequencing primers
724 listed in **Table S6**. The sequencing was performed at the Max-Planck Institute for Evolutionary
725 Biology (Plön, Germany). Sequencing results were assembled and analysed with Geneious Prime
726 (version 2020.1.2).
727
728 **Data availability**
729 *Whole-genome and Sanger sequencing results*. Complete genomes of *E. coli* C WT and ΦX174 WT used as
730 references and raw sequencing reads used to generate **Tables S1 to S5** have been deposited in Zenodo
731 (doi: 10.5281/zenodo.6952399). *Growth curves*. Raw OD measurements used to generate **Fig. S4** have
732 been deposited in Zenodo (doi: 10.5281/zenodo.6952399). *Hierarchical agglomerative clustering and*

heatmap data. Pictures and raw data used to generate **Figs. 6** and **S3** have been deposited in Zenodo (doi: 10.5281/zenodo.6952399).

Additional contact information

Jordan Romeyer Dherbey: dherbey@evolbio.mpg.de – ORCID: 0000-0002-6125-1722 – + 49 4522 763-278

Lavisha Parab: parab@evolbio.mpg.de – ORCID: 0000-0002-7626-3216 – + 49 4522 763-229

Jenna Gallie: gallie@evolbio.mpg.de – ORCID: 0000-0003-2918-0925 – + 49 4522 763-574

Frederic Bertels: bertels@evolbio.mpg.de – ORCID: 0000-0001-6222-4139 – + 49 4522 763-222

Contributions

J.R.D and F.B conceived the study and planned the experiments. J.R.D and L.P. carried out the experiments. J.R.D conducted the sequence analyses. J.R.D, F.B, and J.G interpreted the results. J.R.D., F.B., and J.G. wrote the manuscript. J.R.D prepared all figures and tables. All authors reviewed and approved the manuscript.

Competing interests

The authors declare no competing interests.

Acknowledgements

We received generous core funding from the Max Planck Society. We thank Loukas Theodosiou for his bioinformatic support, David Rogers for troubleshooting PCRs, and Sven Kuenzel for his help with phage and bacterial genome sequencing. We also thank the two reviewers for their time and insightful comments on the manuscript.

763 **References**

764 Amor K, Heinrichs DE, Frirdich E, Ziebell K, Johnson RP, Whitfield C. 2000. Distribution of core
765 oligosaccharide types in lipopolysaccharides from *Escherichia coli*. *Infect Immun.* 68:1116–1124.

766 Bailey MJA, Hughes C, Koronakis V. 1997. RfaH and the *ops* element, components of a novel system
767 controlling bacterial transcription elongation. *Mol Microbiol.* 26:845–851.

768 Barrell BG, Air GM, Hutchison CA. 1976. Overlapping genes in bacteriophage ΦX174. *Nature*
769 264:34–41.

770 Barrett RDH, Schluter D. 2008. Adaptation from standing genetic variation. *Trends Ecol Evol.* 23:38–
771 44.

772 Barrick JE, Colburn G, Deatherage DE, Traverse CC, Strand MD, Borges JJ, Knoester DB, Reba A,
773 Meyer AG. 2014. Identifying structural variation in haploid microbial genomes from short-
774 read resequencing data using *breseq*. *BMC Genomics.* 15:1039.

775 Bearden CM, Agarwal A, Book BK, Vieira CA, Sidner RA, Ochs HD, Young M, Pescovitz MD. 2005.
776 Rituximab inhibits the *in vivo* primary and secondary antibody response to a neoantigen,
777 bacteriophage ΦX174. *Am J Transplant.* 5:50–57.

778 Bertels F, Leemann C, Metzner KJ, Regoes RR. 2019. Parallel evolution of HIV-1 in a long-term
779 experiment. *Mol Biol Evol.* 36:2400–2414.

780 Bertels F, Metzner KJ, Regoes R. 2021. Convergent evolution as an indicator for selection during
781 acute HIV-1 infection. *Peer Community J.* 1:e4.

782 Bertozzi Silva J, Storms Z, Sauvageau D. 2016. Host receptors for bacteriophage adsorption. *FEMS*
783 *Microbiol Lett.* 363:fnw002.

784 Bono LM, Gensel CL, Pfennig DW, Burch CL. 2012. Competition and the origins of novelty:
785 experimental evolution of niche-width expansion in a virus. *Biol Lett.* 9:20120616–20120616.

786 Broeker NK, Barbirz S. 2017. Not a barrier but a key: how bacteriophages exploit host's O-antigen as
787 an essential receptor to initiate infection. *Mol Microbiol.* 105:353–357.

788 Bull JJ, Badgett MR, Wichman HA, Huelsenbeck JP, Hillis DM, Gulati A, Molineux IJ. 1997.
789 Exceptional convergent evolution in a virus. *Genetics.* 147:1497–1507.

790 Bull JJ, Levin BR, Molineux IJ. 2019. Promises and pitfalls of *in vivo* evolution to improve phage
791 therapy. *Viruses.* 11:1083.

792 Burmeister AR, Lenski RE, Meyer JR. 2016. Host coevolution alters the adaptive landscape of a virus.
793 *Proc R Soc B Biol Sci.* 283:20161528.

794 Centers for Disease Control and Prevention (U.S.). 2019. Antibiotic resistance threats in the United
795 States, 2019. Available from: https://stacks.cdc.gov/view/cdc/82532.

796 Chan BK, Turner PE, Kim S, Mojibian HR, Elefteriades JA, Narayan D. 2018. Phage treatment of an
797 aortic graft infected with *Pseudomonas aeruginosa*. *Evol Med Public Health.* 2018:60–66.

798 Colavecchio A, Cadieux B, Lo A, Goodridge LD. 2017. Bacteriophages contribute to the spread of
799 antibiotic resistance genes among foodborne pathogens of the *Enterobacteriaceae* family – A
800 review. *Front Microbiol.* 8:1108.

801 Cox J, Putonti C. 2010. Mechanisms responsible for a ΦX174 mutant's ability to infect *Escherichia coli*
802 by phosphorylation. *J Virol.* 84:4860–4863.

803 Crill WD, Wichman HA, Bull JJ. 2000. Evolutionary reversals during viral adaptation to alternating
804 hosts. *Genetics.* 154:27–37.

805 Deatherage DE, Barrick JE. 2014. Identification of mutations in laboratory-evolved microbes from
806 next-generation sequencing data using *breseq*. *Methods Mol Biol.* 1151:165–188.

807 Deatherage DE, Traverse CC, Wolf LN, Barrick JE. 2015. Detecting rare structural variation in
808 evolving microbial populations from new sequence junctions using *breseq*. *Front Genet.* 5:468.

809 Eisenberg S, Ascarelli R. 1981. The A* protein of ΦX174 is an inhibitor of DNA replication. *Nucleic*
810 *Acids Res.* 9:1991–2002.

811 Feige, Ulrich, Stirm, Stephan. 1976. On the structure of *Escherichia coli* C cell wall lipopolysaccharide
812 core and its ΦX174 receptor region. *Biochem Biophys Res Commun.* 71:8.

813 Gupta A, Zaman L, Strobel HM, Gallie J, Burmeister AR, Kerr B, Tamar ES, Kishony R, Meyer JR.
814 2022. Host-parasite coevolution promotes innovation through deformations in fitness
815 landscapes. *eLife.* 11:e76162.

816 Hancock RE, Reeves P. 1976. Lipopolysaccharide-deficient, bacteriophage-resistant mutants of
817 *Escherichia coli* K-12. *J Bacteriol.* 127:98–108.

818 Hermisson J, Pennings PS. 2005. Soft sweeps: molecular population genetics of adaptation from
819 standing genetic variation. *Genetics.* 169:2335–2352.

820 Inagaki M, Tanaka A, Suzuki R, Wakashima H, Kawaura T, Karita S, Nishikawa S, Kashimura N.
821 2000. Characterization of the binding of spike H protein of bacteriophage ΦX174 with
822 receptor lipopolysaccharides. *J Biochem.* 127:577–583.

823 Incardona NL, Selvidge L. 1973. Mechanism of adsorption and eclipse of bacteriophage ΦX174. II.
824 Attachment and eclipse with isolated *Escherichia coli* cell wall lipopolysaccharide. *J Virol.*
825 11:775–782.

826 Incardona NL, Tuech JK, Murti G. 1985. Irreversible binding of phage ΦX174 to cell-bound
827 lipopolysaccharide receptors and release of virus-receptor complexes. *Biochemistry.* 24:6439–
828 6446.

829 Jamet A, Touchon M, Ribeiro-Gonçalves B, Carriço JA, Charbit A, Nassif X, Ramirez M, Rocha EPC.
830 2017. A widespread family of polymorphic toxins encoded by temperate phages. *BMC Biol.*
831 15:75.

832 Kawaura T, Inagaki M, Karita S, Kato M, Nishikawa S, Kashimura N. 2000. Recognition of receptor
833 lipopolysaccharides by spike G protein of bacteriophage ΦX174. *Biosci Biotechnol Biochem.*
834 64:1993–1997.

835 Klein G, Müller-Loennies S, Lindner B, Kobylak N, Brade H, Raina S. 2013. Molecular and structural
836 basis of inner core lipopolysaccharide alterations in *Escherichia coli*: incorporation of glucuronic
837 acid and phosphoethanolamine in the heptose region. *J Biol Chem.* 288:8111–8127.

838 Klein G, Raina S. 2019. Regulated assembly of LPS, its structural alterations and cellular response to
839 LPS defects. *Int J Mol Sci.* 20:356.

840 Kneidinger B, Marolda C, Graninger M, Zamyatina A, McArthur F, Kosma P, Valvano MA, Messner
841 P. 2002. Biosynthesis pathway of ADP-L-glycero-β-D-manno-heptose in *Escherichia coli*. *J*
842 *Bacteriol.* 184:7.

843 Kojima H, Inagaki M, Tomita T, Watanabe T. 2010. Diversity of non-stoichiometric substitutions on
844 the lipopolysaccharide of *E. coli* C demonstrated by electrospray ionization single quadrupole
845 mass spectrometry. *Rapid Commun Mass Spectrom.* 24:43–48.

846 Król JE, Hall DC, Balashov S, Pastor S, Sibert J, McCaffrey J, Lang S, Ehrlich RL, Earl J, Mell JC, et
847 al. 2019. Genome rearrangements induce biofilm formation in *Escherichia coli* C – an old model
848 organism with a new application in biofilm research. *BMC Genomics.* 20:767.

849 Krüger A, Lucchesi PMA. 2015. Shiga toxins and stx phages: highly diverse entities. *Microbiol Read*
850 *Engl.* 161:451–462.

851 Kulikov EE, Golomidova AK, Prokhorov NS, Ivanov PA, Letarov AV. 2019. High-throughput LPS
852 profiling as a tool for revealing of bacteriophage infection strategies. *Sci Rep.* 9:2958.

853 Labrie SJ, Samson JE, Moineau S. 2010. Bacteriophage resistance mechanisms. *Nat Rev Microbiol.*
854 8:317–327.

855 Latino L, Midoux C, Hauck Y, Vergnaud G, Pourcel C. 2016. Pseudolysogeny and sequential
856 mutations build multiresistance to virulent bacteriophages in *Pseudomonas aeruginosa*. *Microbiol*
857 *Read Engl.* 162:748–763.

858 van der Ley P, de Graaff P, Tommassen J. 1986. Shielding of *Escherichia coli* outer membrane proteins
859 as receptors for bacteriophages and colicins by O-antigenic chains of lipopolysaccharide. *J*
860 *Bacteriol.* 168:449–451.

861 Lind PA, Libby E, Herzog J, Rainey PB. 2019. Predicting mutational routes to new adaptive
862 phenotypes. *eLife.* 8:e38822.

863 Luria SE, Delbrück M. 1943. Mutations of bacteria from virus sensitivity to virus resistance. *Genetics.*
864 28:491–511.

865 Maldonado RF, Sá-Correia I, Valvano MA. 2016. Lipopolysaccharide modification in Gram-negative
866 bacteria during chronic infection. *FEMS Microbiol Rev.* 40:480–493.

867 Matsuura M. 2013. Structural modifications of bacterial lipopolysaccharide that facilitate Gram-
868 Negative bacteria evasion of host innate immunity. *Front Immunol.* 4:109.

869 McArthur F, Andersson CE, Loutet S, Mowbray SL, Valvano MA. 2005. Functional analysis of the
870 glycero-manno-heptose 7-phosphate kinase domain from the bifunctional HldE protein,
871 which is involved in ADP-L-glycero-D-manno-heptose biosynthesis. *J Bacteriol.* 187:5292–
872 5300.

873 McKenna R, Xia D, Willingmann P, Ilag LL, Krishnaswamy S, Rossmann MG, Olson NH, Baker TS,
874 Incardona NL. 1992. Atomic structure of single-stranded DNA bacteriophage ΦX174 and its
875 functional implications. *Nature.* 355:137–143.

876 Meyer JR, Dobias DT, Weitz JS, Barrick JE, Quick RT, Lenski RE. 2012. Repeatability and
877 contingency in the evolution of a key innovation in phage Lambda. *Science.* 335:428–432.

878 Michel A, Clermont O, Denamur E, Tenaillon O. 2010. Bacteriophage ΦX174's ecological niche and
879 the flexibility of its *Escherichia coli* lipopolysaccharide receptor. *Appl Environ Microbiol.* 76:7310–
880 7313.

881 Monteiro R, Pires DP, Costa AR, Azeredo J. 2019. Phage therapy: going temperate? *Trends Microbiol.*
882 27:368–378.

883 Moxon ER, Rainey PB, Nowak MA, Lenski RE. 1994. Adaptive evolution of highly mutable loci in
884 pathogenic bacteria. *Curr Biol.* 4:24–33.

885 Murray CJ, Ikuta KS, Sharara F, Swetschinski L, Aguilar GR, Gray A, Han C, Bisignano C, Rao P,
886 Wool E, et al. 2022. Global burden of bacterial antimicrobial resistance in 2019: a systematic
887 analysis. *The Lancet.* 399:629–655.

888 Mutalik VK, Adler BA, Rishi HS, Piya D, Zhong C, Koskella B, Kutter EM, Calendar R, Novichkov
889 PS, Price MN, et al. 2020. High-throughput mapping of the phage resistance landscape in *E.*
890 *coli. PLOS Biol.* 18:e3000877.

891 Nikaido H. 2003. Molecular basis of bacterial outer membrane permeability revisited. *Microbiol Mol*
892 *Biol Rev.* 67:593–656.

893 Oechslin F. 2018. Resistance development to bacteriophages occurring during bacteriophage therapy.
894 *Viruses.* 10:351.

895 Pagnout C, Sohm B, Razafitianamaharavo A, Caillet C, Offroy M, Leduc M, Gendre H, Jomini S,
896 Beaussart A, Bauda P, et al. 2019. Pleiotropic effects of *rfa*-gene mutations on *Escherichia coli*
897 envelope properties. *Sci Rep.* 9:9696.

898 Picelli S, Björklund ÅK, Reinius B, Sagasser S, Winberg G, Sandberg R. 2014. Tn5 transposase and
899 tagmentation procedures for massively scaled sequencing projects. *Genome Res.* 24:2033–2040.

900 Qian J, Garrett TA, Raetz CRH. 2014. *In vitro* assembly of the outer core of the lipopolysaccharide
901 from *Escherichia coli* K-12 and *Salmonella typhimurium. Biochemistry.* 53:1250–1262.

902 Raetz CRH, Whitfield C. 2002. Lipopolysaccharide endotoxins. *Annu Rev Biochem.* 71:635–700.

903 Ramirez J, Guarner F, Bustos Fernandez L, Maruy A, Sdepanian VL, Cohen H. 2020. Antibiotics as
904 major disruptors of gut microbiota. *Front Cell Infect Microbiol.* 10:572912

905 Remold SK, Rambaut A, Turner PE. 2008. Evolutionary genomics of host adaptation in vesicular
906 stomatitis virus. *Mol Biol Evol.* 25:1138–1147.

907 Rokyta DR, Burch CL, Caudle SB, Wichman HA. 2006. Horizontal gene transfer and the evolution
908 of microvirid coliphage genomes. *J Bacteriol.* 188:1134–1142.

909 Rubinstein A, Mizrachi Y, Bernstein L, Shliozberg J, Golodner M, Liu GQ, Ochs HD. 2000.
910 Progressive specific immune attrition after primary, secondary and tertiary immunizations with
911 bacteriophage ΦX174 in asymptomatic HIV-1 infected patients. *AIDS Lond Engl.* 14:F55-62.

912 Sanger, Coulsox AR, Friedmax T, Barrell BG, Browns L, Fiddes JC, Hctchisos CA, Sloconbe PM,
913 Switi M. 1978. The nucleotide sequence of bacteriophage ΦX174. *J Mol Biol.* 125:225–246.

914 Sant DG, Woods LC, Barr JJ, McDonald MJ. 2021. Host diversity slows bacteriophage adaptation by
915 selecting generalists over specialists. *Nat Ecol Evol.* 5:350–359.

916 Schnaitman CA, Klena JD. 1993. Genetics of lipopolysaccharide biosynthesis in enteric bacteria.
917 *Microbiol Rev.* 57:655–682.

918 Seregina TA, Petrushanko IY, Shakulov RS, Zaripov PI, Makarov AA, Mitkevich VA, Mironov AS.
919 2022. The inactivation of LPS biosynthesis genes in *E. coli* cells leads to oxidative stress. *Cells.*
920 11:2667.

921 Simpson BW, Trent MS. 2019. Pushing the envelope: LPS modifications and their consequences. *Nat*
922 *Rev Microbiol.* 17:403–416.

923 Sinsheimer RL. 1959. A single-stranded deoxyribonucleic acid from bacteriophage ΦX174. *J Mol Biol.*
924 1:43–53.

925 Sun Y, Roznowski AP, Tokuda JM, Klose T, Mauney A, Pollack L, Fane BA, Rossmann MG. 2017.
926 Structural changes of tailless bacteriophage ΦX174 during penetration of bacterial cell walls.
927 *Proc Natl Acad Sci.* 114:13708–13713.

928 Valvano MA, Marolda CL, Bittner M, Glaskin-Clay M, Simon TL, Klena JD. 2000. The *rfaE* gene
929 from *Escherichia coli* encodes a bifunctional protein involved in biosynthesis of the
930 lipopolysaccharide core precursor ADP-L-glycero-D-manno-heptose. *J Bacteriol.* 182:488–497.

931 Weisbeek PJ, Van de Pol JH, Van Arkel GA. 1973. Mapping of host range mutants of bacteriophage
932 ΦX174. *Virology.* 52:408–416.

933 Whitfield C, Heinrichs DE, Yethon JA, Amor KL, Monteiro MA, Perry MB. 1999. Assembly of the
934 R1-type core oligosaccharide of *Escherichia coli* lipopolysaccharide. 5:151–156.

935 WHO. 2021. Antimicrobial resistance. Available from: https://www.who.int/news-room/fact-
936 sheets/detail/antimicrobial-resistance

937 Wichman HA, Badgett MR, Scott LA, Boulianne CM, Bull JJ. 1999. Different trajectories of parallel
938 evolution during viral adaptation. *Science* .285:422–424.

939 Yethon JA, Heinrichs DE, Monteiro MA, Perry MB, Whitfield C. 1998. Involvement of *waaY*, *waaQ*,
940 and *waaP* in the modification of *Escherichia coli* lipopolysaccharide and their role in the
941 formation of a stable outer membrane. *J Biol Chem.* 273:26310–26316.

942 Yethon JA, Vinogradov E, Perry MB, Whitfield C. 2000. Mutation of the lipopolysaccharide core
943 glycosyltransferase encoded by *waaG* destabilizes the outer membrane of *Escherichia coli* by
944 interfering with core phosphorylation. *J Bacteriol.* 182:5620–5623.

945 Zhang G, Meredith TC, Kahne D. 2013. On the essentiality of lipopolysaccharide to Gram-negative
946 bacteria. *Curr Opin Microbiol.* 16:779–785.

947

Supplementary Text S1

Excluded bacteria and phage isolates from downstream analyses. We removed four bacterial strains (*E. coli* C R1, R3, R15, and R19) and two evolved phage strains (ΦX174 R5 T2 and ΦX174 R19 T1) from both mutational and phenotypical analyses. The reasons behind these exclusions are outlined below.

Bacteria. We found that both *E. coli* C R3 and R15's glycerol stocks contain more than one genotype; while whole genome re-sequencing from their respective glycerol stocks showed only a single mutation in *galE*, whole genome re-sequencing of ten re-streaked colonies showed that additional mutations were systematically associated with the single mutation in *galE* (**Tables S4 and S5**). *E. coli* C R1 displayed an unstable resistant phenotype using the spotting assay *method 1* (see section **Determination of the evolved phages' host range by spotting assays**). We performed phenotypic assays in a semi-solid environment by plating top agar overlays from overnight cultures of *E. coli* C R1 without phage. All overnight cultures were started with a randomly picked single colony obtained from the glycerol stock of R1. We observed that colonies of R1 made different lawn types: either "smooth" (no bacterial aggregate) or "granulous" (presence of numerous bacterial aggregates), which could potentially impact phage infectivity. The existence of two different aggregation phenotypes suggests that the glycerol stock of *E. coli* C R1 consists of two different populations. Unlike R3 and R15, however, no discrepancy was found between the whole genome re-sequencing results of R1 from the glycerol stock and its ten re-streaked colonies. The exact cause of the phenotypic inconsistency could not be identified. *E. coli* C R19 remains sensitive to ΦX174 wildtype infection. When plated undiluted, a high titer ΦX174 wildtype lysate (~10^9 pfu ml^{-1}) could not clear *E. coli* C R19's lawn, but a few thousand small clear plaques were produced. Thus, R19 is likely to be only partially resistant to ΦX174 wildtype infection. It carries a single mutation *yajC* (locus tag B6N50_17610), which encodes a periplasmic protein (Fang and Wei 2011) with a putative preprotein translocase subunit (Pfam e-value 2.3e-26) (see **Table S4**). While no link to the LPS biosynthesis or assembly has been defined yet, *yajC* could conceivably play a role in the injection of phage DNA into the bacterium's cytoplasmic membrane (Schulze et al. 2014; Bohm et al. 2018).

In our matrices (**Figs. 6 and S3**), *E. coli* C R32 cannot be infected by any evolved phages from the first evolution experiment. The phage infecting R5 was the only phage that could infect R32 but was removed from the subsequent analysis (see below).

33

34 *Phage*. We removed the evolved phage infecting R5 (ΦX174 R5 T2) because its glycerol stock contains
35 more than one genotype (confirmed by Sanger Sequencing). Since we removed R19 from the final
36 analysis, we also removed its corresponding evolved phage obtained during the first evolution
37 experiment (ΦX174 R19 T1). Details on their respective mutations (in the *H* gene) can be found in
38 **Table S4**.

39

40

41 ## Supplementary Figures

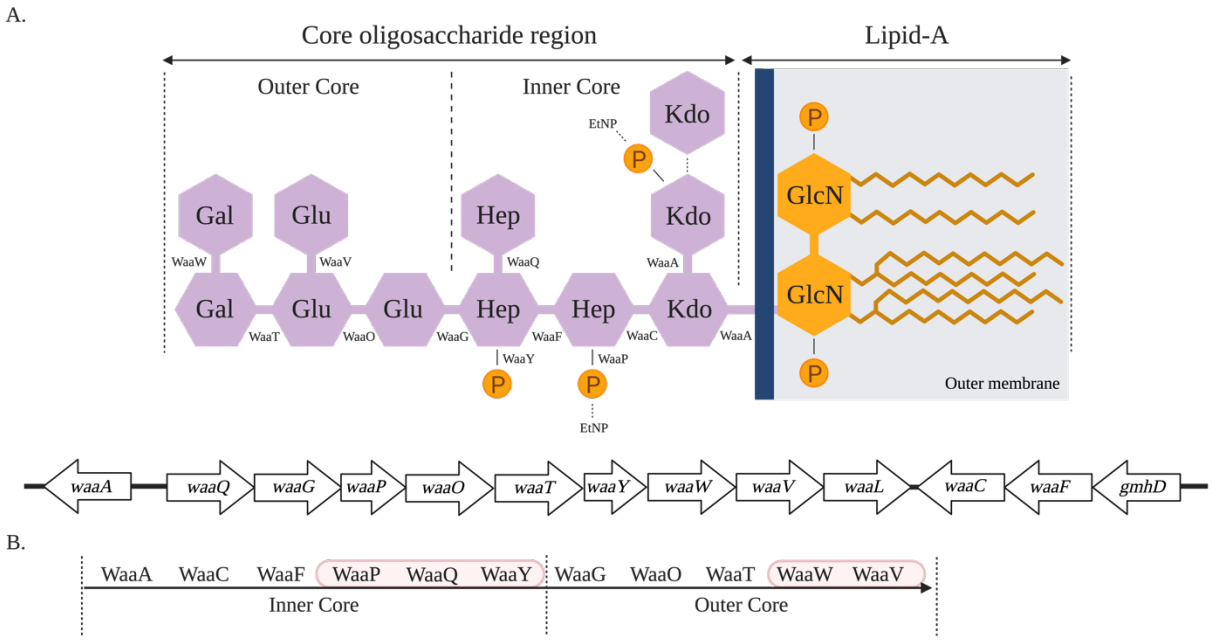

42

43

44 **Fig. S1. Assembly of *E. coli* rough type core LPS. A.** Organization of the chromosomal *waa* region
45 in the *E. coli C* wildtype strain. The chromosomal *waa* locus (formerly named *rfa*) is organized into
46 three major operons, usually designated by the first gene of each transcriptional unit: *waaA, gmhD* and
47 *waaQ* (Whitfield et al. 1999). The *waaA* operon is responsible for the incorporation of two Kdo (3-
48 deoxy-D-*manno*-octulosonic acids) moieties to the lipid A (Belunis et al. 1995). The *gmhD* operon is
49 required for the assembly of the inner core's backbone (Schnaitman and Klena 1993), and the *waaQ*
50 operon contains all eight genes necessary to modify the inner core and built the outer core (Whitfield
51 et al. 1999) **B.** Sequential steps of the core OS LPS synthesis (from WaaA to WaaV). *Inner core assembly*
52 *and modification*. Inner core assembly starts first with WaaA adding the two Kdo moieties to the lipid-
53 A-IV precursor (Schnaitman and Klena 1993; Whitfield et al. 1999; Amor et al. 2000). A bacterium
54 lacking WaaA activity displays severe membrane defects, resulting in the inability to form colonies
55 (Klein et al. 2009). Heptose residues I and II are then anchored to the Kdo moieties by the
56 heptosyltransferases WaaC and WaaF, respectively (Jansson et al. 1981; Schnaitman and Klena 1993;
57 Whitfield et al. 1999). LPS core heptose kinases WaaP and WaaY add phosphate groups to the first
58 and second heptose residues, respectively. WaaQ adds the last heptose to the second heptose residue
59 (Jansson et al. 1981; Schnaitman and Klena 1993; Whitfield et al. 1999). *WaaP*, *waaQ*, and *waaY*
60 proceed in this specific order. *WaaY* cannot work without the activity of *waaQ*, which cannot work

without *waaP* (first red ellipse). *Outer core assembly*. The glucosyltransferases WaaG and WaaO start the formation of the outer core by anchoring the first glucose to the second heptose residue and the second glucose to the first glucose residue, respectively (Heinrichs, Yethon, and Whitfield 1998; Vinogradov et al. 1999; Whitfield et al. 1999). It has been suggested that the WaaG-catalyzed reaction might be required for WaaP and WaaY substrate specificity (Yethon et al. 2000). Then, the galactosyltransferases WaaT and WaaW add the first galactose to the second glucose residue and the second galactose to the first galactose residue, respectively (Heinrichs, Yethon, Amor, et al. 1998; Whitfield et al. 1999). The completion of the outer core LPS is achieved when WaaV adds the third glucose to the second glucose residue. Here, *waaV* requires the activity of *waaW* and proceeds in this specific order (second red ellipse). If *waaW* is deleted, *waaV* is not functional (Heinrichs, Yethon, Amor, et al. 1998; Leipold et al. 2007). Modifications of the LPS structure can lead to major phenotypic effects. In particular, the deep rough phenotype is usually associated with a strongly destabilized outer membrane, a decreased expression of some outer membrane proteins, a modification of the turgor pressure (Pagnout et al. 2019), and an increase of susceptibility to hydrophobic compounds such as AMPs (antimicrobial peptides), antibiotics, or bacteriocins (van der Ley et al. 1986; Schnaitman and Klena 1993; Yethon et al. 1998; Whitfield et al. 1999; Amor et al. 2000; Klein et al. 2013). Differences in LPS structures can also affect interactions with the host immune system (Raetz and Whitfield 2002; Matsuura 2013) and phage resistance (Hancock and Reeves 1976; Labrie et al. 2010; Kulikov et al. 2019; Mutalik et al. 2020).

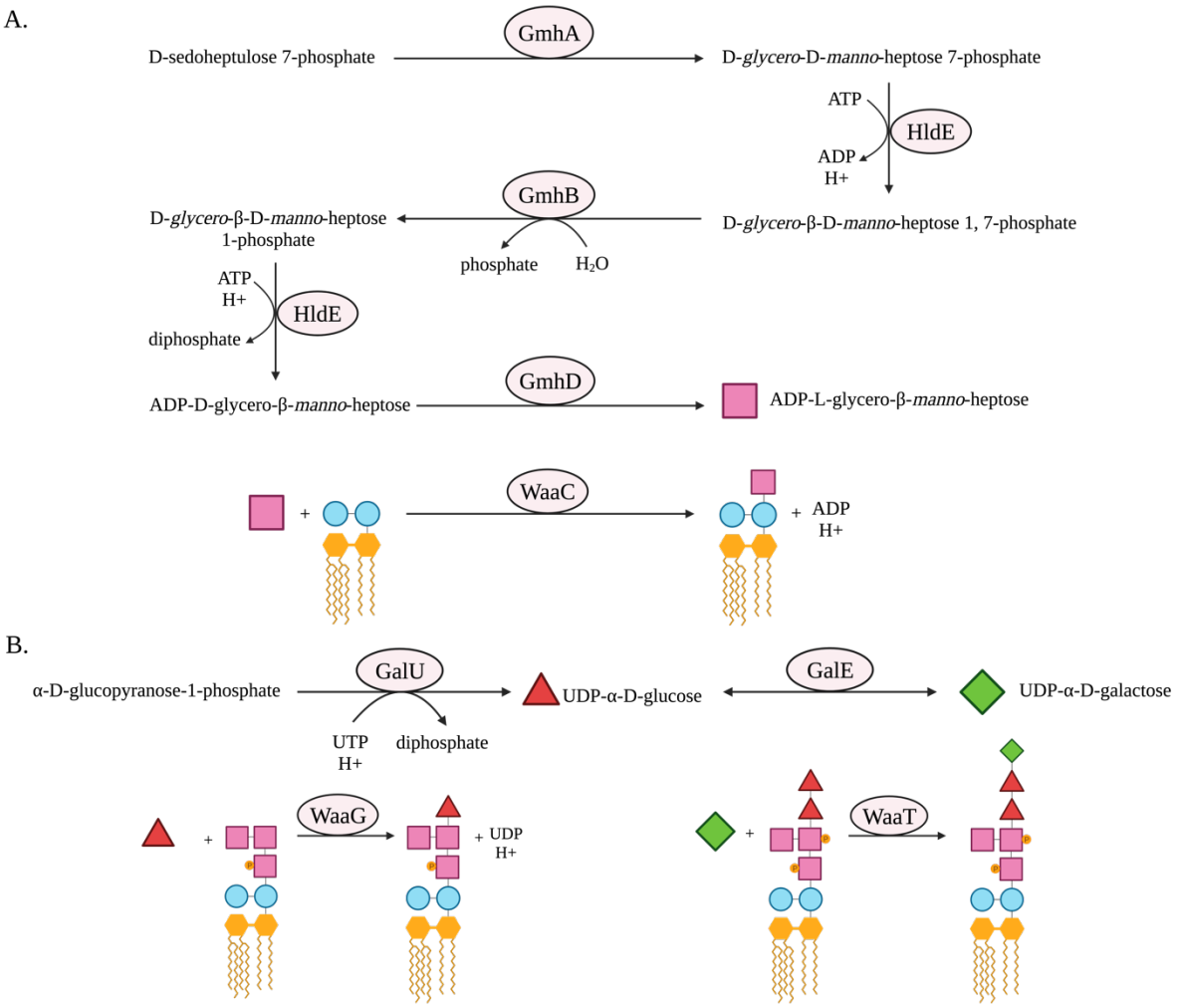

Fig S2. Biosynthesis of the core LPS glucose, galactose and heptose sugar components. A. ADP-L-glycero-β-D-*manno*-heptose synthesis pathway. It involves four genes: *gmhA*, *hldE*, *gmhB* and *gmhD*. Each gene encodes a protein that catalyses the production of a heptose intermediate. The final product is ADP-L-glycero-β-D-*manno*-heptose, which is used by the heptosyltransferase WaaC to build the inner core LPS (Kneidinger et al. 2002). Thus, deletion of one of these genes is expected to result in an heptoseless, deep rough LPS (McArthur et al. 2005). This figure is adapted from https://biocyc.org/ECOLI/NEW-IMAGE?type=PATHWAY&object=PWY0-1241 (Karp et al. 2019). **B.** Galactose degradation I (Leloir Pathway). GalU and GalE function in the Leloir pathway (Frey 1996; Kneidinger et al. 2002; McArthur et al. 2005). GalU catalyses the formation of UDP-α-D-glucose from α-D-glucopyranose 1- phosphate (Weissborn et al. 1994). UDP-α-D-glucose can then be incorporated into the outer core LPS by WaaG. Therefore, both Δ*galU* and Δ*waaG* mutants result

in the same truncated LPS structure (Schnaitman and Klena 1993; Weissborn et al. 1994; Genevaux et al. 1999). GalE catalyses the interconversion of UDP-α-D-galactose and UDP-α-D-glucose during galactose catabolism (Pierson and Carlson 1996). UDP-α-D-galactose is then incorporated into the outer core LPS by WaaT (Heinrichs, Yethon, Amor, et al. 1998). Therefore, both Δ*galE* and Δ*waaT* are expected to result in the same truncated LPS (Schnaitman and Austin 1990). This figure was adapted from https://biocyc.org/ECOLI/NEW-IMAGE?type=PATHWAY&object=GALACTMETAB-PWY (Karp et al. 2019).

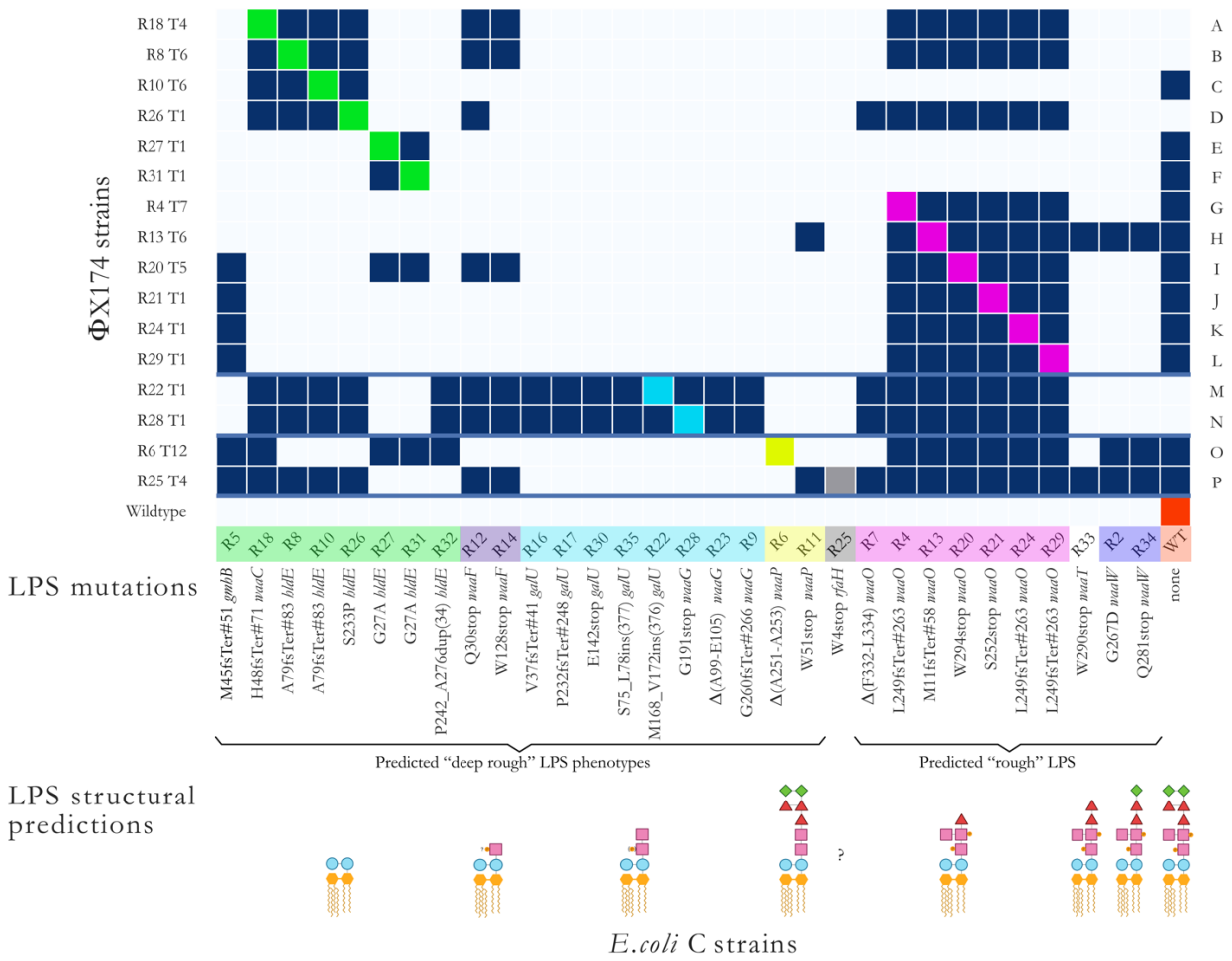

Fig. S3. Infection matrix of evolved ΦX174 phages on the 31 resistant *E. coli* C strains. The infection matrix was produced by combining the results of two spotting methods and the plaque assays (see **Methods**). *E. coli* C R32 cannot be infected by any evolved phages from the first phage evolution experiment. The phage infecting R5 was the only phage that could infect R32 (**Text S1**) but was removed from the subsequent analysis due to a lack of isogeny. *E. coli* C strains are grouped and coloured based on their predicted core LPS structures (Jansson et al. 1981; Schnaitman and Austin 1990; Schnaitman and Klena 1993; Weissborn et al. 1994; Heinrichs, Yethon, and Whitfield 1998; Genevaux et al. 1999; Vinogradov et al. 1999; Whitfield et al. 1999; Amor et al. 2000; Kawaura et al. 2000; Yethon et al. 2000; Kneidinger et al. 2002; Raetz and Whitfield 2002; McArthur et al. 2005; Leipold et al. 2007; Fang and Wei 2011; Król et al. 2019). ΦX174 strains are ordered based on the predicted LPS structures they infected during the evolution experiments (A-F: overcame heptoseless *waaC* and *hldE* mutants; G-L: overcame *waaO* mutants; M-N: overcame *galU* and *waaG* mutants; O:

116 overcame *waaP*/*pssA* mutant; P: overcame *rfaH* mutant). The solid blue lines separate the evolved
117 phages according to the evolution experiment in which they were isolated (A-L: first; M-N: second;
118 O-P: third). Dark blue squares=infection, light blue square=no infection, coloured square=control
119 infection by a phage evolved on that host. R# indicates the number of the resistant strain the phage
120 evolved on, and T# is the transfer number where plaques were first observed. "?": core LPS structure
121 of *E. coli* C R25 (*rfaH* mutant) could not be predicted. "INS": insertion. "DUP": duplication. "stop":
122 stop codon. "Δ": deletion. Examples: L249fsTer#263 indicates a frameshift (fs) leading to a premature
123 codon stop (Ter); the position of the premature stop codon is in parentheses. S75_L78ins(377)
124 indicates an insertion; the two flanking amino acids are separated by a "_" and followed by the number
125 of inserted amino acids in parentheses. Δ(A99-E105) indicated deletion; two flanking amino acids are
126 separated by a "-". P242_A276dup(34) indicates a duplication; the two flanking amino acids are
127 separated by a "_" and followed by the number of duplicated amino acids in parentheses.
128

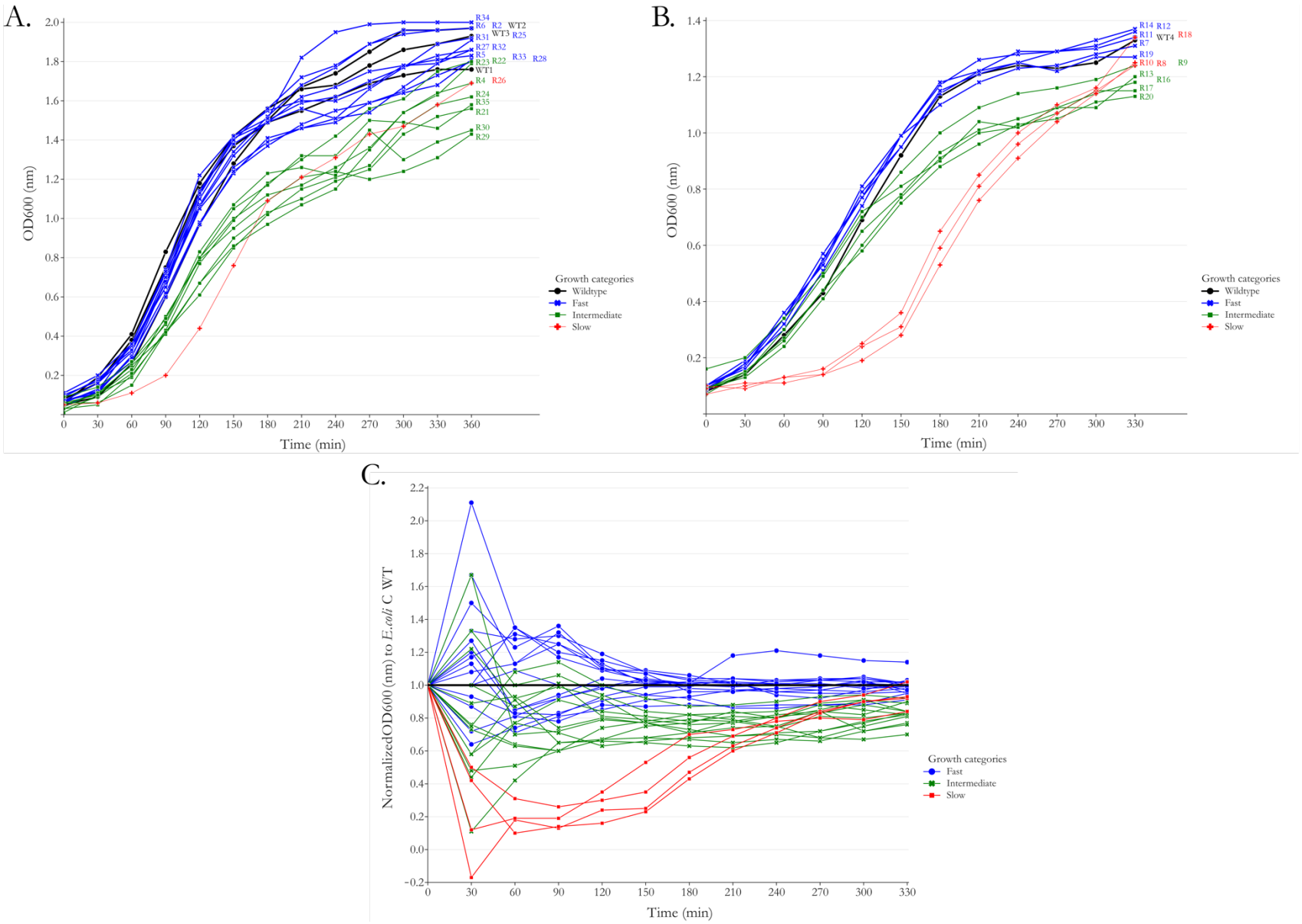
A.
OD600 (nm)
Time (min)
R34
R6
R2
WT2
WT3
R25
R31
R27
R32
R5
R33
R28
R23
R22
WT1
R4
R26
R24
R35
R21
R30
R29
Growth categories
Wildtype
Fast
Intermediate
Slow
B.
OD600 (nm)
Time (min)
R14
R12
R11
WT4
R18
R7
R19
R10
R8
R9
R13
R16
R17
R20
Growth categories
Wildtype
Fast
Intermediate
Slow
C.
NormalizedOD600 (nm) to E.coli C WT
Time (min)
Growth categories
Fast
Intermediate
Slow

129

130 **Fig. S4. *E. coli* C resistant strains can be categorized as fast, intermediate, or slow growers.** The mean OD600 values of two
131 independent cultures grown in 5 ml LB at each time point for each bacterial mutant were calculated and plotted. Resistant strains are
132 categorized with respect to their growth compared to *E. coli* C wildtype. Black lines: *E. coli* C wildtype. Blue lines: resistant bacteria that grew
133 similarly to *E. coli* C wildtype ("fast growers"). Green lines: resistant strains grew somewhat more slowly than *E. coli* C wildtype and fast
134 growers ("intermediate growers"). Red lines: resistant strains that grew more slowly than *E. coli* C wildtype and intermediate growers ("slow
135 growers"). **A.** Growth curves of resistant strains R2-R6 and R21-R35. **B.** Growth curves of resistant strains R7-R20. These data (mutants
136 and controls) were collected in a separate block to those in panel A. **C.** Mean OD600 values of all resistant strains in panels A and B, each
137 normalized with respect to their corresponding *E. coli* C wildtype control $((OD600_R\#_{ti} - ODR\#_{t0})/(OD600_wildtype_{ti} -$
138 $OD600_wildtype_{t0}))$. R# is the resistant strain number.
139

140

Supplementary Tables

E. coli C resistant strains	Genes	Locus tags	Synonyms	Descriptions	Positions	Nucleotide changes	Amino Acid changes	Predicted LPS structure phenotypes	"Easy" or "Hard" LPS structure phenotypes?	# Experiment during which resistance was overcome or cross-infected
R2	*waaW*	*B6N50_00430* →	-	UDP-galactose--(galactosyl) LPS alpha1,2-galactosyltransferase	79,779	g→a	G267D	Rough	Easy	1
R4	*waaO*	*B6N50_00415* →	*rfaI*	UDP-D-glucose:(glucosyl) LPS α-1,3-glucosyltransferase	76,970	$(a)_{7\rightarrow6}$	L249fsTer#263[a]	Rough	Easy	1
R5	*gmhB*	*B6N50_18960* ←	-	D-glycero-β-D-manno-heptose 1,7-bisphosphate 7-phosphatase	3,693,747	$(t)_{8\rightarrow7}$	M45fsTer#51	Deep rough	Easy	1
R6	*waaP*	*B6N50_00410* →	*rfaP*	Lipopolysaccharide core heptose(I) kinase	76,163 - 76,168	Δ6 bp	Δ(A251-A253)	Deep rough	Hard	3
	pssA	*B6N50_06070* ←	-	Phosphatidylserine synthase	1,190,560	t→g	V54V			
R7	*waaO*	*B6N50_00415* →	*rfaI*	UDP-D-glucose:(glucosyl) LPS α-1,3-glucosyltransferase	77,219 - 77,224	$(ttattt)_{2\rightarrow1}$	Δ(F332-L334)	Rough	Easy	1
R8	*hldE*	*B6N50_03700* →	*rfaE/waaE*	Bifunctional heptose 7-phosphate kinase/heptose 1-phosphate adenyltransferase	721,891 - 721,892	$(gc)_{5\rightarrow4}$	A79fsTer#83	Deep rough	Easy	1
R9	*waaG*	*B6N50_00405* →	*rfaG*	UDP-glucose:(heptosyl) LPS α1,3-glucosyltransferase (glucosyltransferase I)	75,073 - 75,076	Δ4 bp	G260fsTer#266	Deep rough	Hard	2
R10	*hldE*	*B6N50_03700* →	*rfaE/waaE*	Bifunctional heptose 7-phosphate kinase/heptose 1-phosphate adenyltransferase	721,891 - 721,892	$(gc)_{5\rightarrow4}$	A79fsTer#83	Deep rough	Easy	1
	CRISPR	*B6N50_05180* → / ← *B6N50_05185*	-	Repeat region	1,023,697 - 1,023,940	Δ244 bp	Non-coding region			
R11	*waaP*	*B6N50_00410* →	*rfaP*	Lipopolysaccharide core heptose(I) kinase	75,562	g→a	W51stop	Deep rough	Easy	1

R12	*waaF*	*B6N50_00450* ←	*rfaF*	ADP-heptose LPS heptosyltransferase II	84,376	g→a	Q30stop	Deep rough	Easy	1
R13	*waaO*	*B6N50_00415* →	*rfaI*	UDP-D-glucose:(glucosyl) LPS α-1,3-glucosyltransferase	76,255	Δ1 bp	M11fsTer#58	Rough	Easy	1
R14	*waaF*	*B6N50_00450* ←	*rfaF*	ADP-heptose LPS heptosyltransferase II	84,081	c→t	W128stop	Deep rough	Easy	1
R16	*galU*	*B6N50_13325* ←	-	UTP--glucose-1-phosphate uridylyltransferase	2,611,994	Δ1 bp	V37fsTer#41	Deep rough	Hard	2
R17	*galU*	*B6N50_13325* ←	-	UTP--glucose-1-phosphate uridylyltransferase	2,611,409	$(g)_{4\rightarrow3}$	P232fsTer#248	Deep rough	Hard	2
R18	*waaC*	*B6N50_00445* ←	*rfaC*	ADP-heptose LPS heptosyltransferase I	83,271	Δ1 bp	H48fsTer#71	Deep rough	Easy	1
R20	*waaO*	*B6N50_00415* →	*rfaI*	UDP-D-glucose:(glucosyl) LPS α-1,3-glucosyltransferase	77,104	g→a	W294stop	Rough	Easy	1
R21	*waaO*	*B6N50_00415* →	*rfaI*	UDP-D-glucose:(glucosyl) LPS α-1,3-glucosyltransferase	76,978	c→a	S252stop	Rough	Easy	1
	potH	*B6N50_15295* ←	-	Spermidine/putrescine ABC transporter permease	2,990,409	g→t	Q310K			
R22	*galU*	*B6N50_13325* ←	-	UTP--glucose-1-phosphate uridylyltransferase	2,611,590 - 2,611,600	INS 2,783,815 - 2,784,943	M168_V172ins(376)[b]	Deep rough	Hard	2
R23	*waaG*	*B6N50_00405* →	*rfaG*	UDP-glucose:(heptosyl) LPS α1,3-glucosyltransferase (glucosyltransferase I)	74,589 - 74,606	Δ18 bp	Δ(A99-E105)	Deep rough	Hard	2
R24	*waaO*	*B6N50_00415* →	*rfaI*	UDP-D-glucose:(glucosyl) LPS α-1,3-glucosyltransferase	76,970	$(a)_{7\rightarrow6}$	L249fsTer#263	Rough	Easy	1
R25	*rfaH*	*B6N50_22865* →	-	Transcription/translation regulatory transformer protein	4,485,876	g→a	W4stop	Unknown	Hard	3
R26	*hldE*	*B6N50_03700* →	*rfaE/waaE*	Bifunctional heptose 7-phosphate kinase/heptose 1-phosphate adenyltransferase	722,353	t→c	S233P	Deep rough	Easy	1

R27	*hldE*	*B6N50_03700* →	*rfaE/waaE*	Bifunctional heptose 7-phosphate kinase/heptose 1-phosphate adenyltransferase	721,736	g→c	G27A	Deep rough	Easy	1
R28	*waaG*	*B6N50_00405* →	*rfaG*	UDP-glucose:(heptosyl) LPS α1,3-glucosyltransferase (glucosyltransferase I)	74,864	g→t	G191stop	Deep rough	Hard	2
R29	*waaO*	*B6N50_00415* →	*rfaI*	UDP-D-glucose:(glucosyl) LPS α-1,3-glucosyltransferase	76,970	$(a)_{7\rightarrow 6}$	L249fsTer#263	Rough	Easy	1
	pcoA	*B6N50_01165* ←	-	Multicopper oxidase	237,963 - 237,973	INS 1,040,936 - 1,042,273	G152_G155ins(446)			
	eutM - *eutN* - *eutE*	*[B6N50_06785]* - *[B6N50_06790]* - *[B6N50_06795]* →	-	Ethanolamine utilization protein EutM - Ethanolamine utilization protein EutN - Aldehyde dehydrogenase EutE	1,342,381 - 1,343,448	Δ1,068 bp	Δ[EutM_A58-EutE_A181][c]			
R30	*galU*	*B6N50_13325* ←	-	UTP--glucose-1-phosphate uridylyltransferase	2,611,680	c→a	E142stop	Deep rough	Hard	2
R31	*hldE*	*B6N50_03700* →	*rfaE/waaE*	Bifunctional heptose 7-phosphate kinase/heptose 1-phosphate adenyltransferase	721,736	g→c	G27A	Deep rough	Easy	1
R32	*hldE*	*B6N50_03700* →	*rfaE/waaE*	Bifunctional heptose 7-phosphate kinase/heptose 1-phosphate adenyltransferase	722,381 - 722,482	DUP 722,381-722,482 (102) bp	P242_A276dup(34)[d]	Deep rough	Easy	1
R33	*waaT*	*B6N50_00420* →	-	UDP-galactose:(glucosyl) LPS α-1,2-galactosyltransferase	78,125	g→a	W290stop	Rough	Easy	1
R34	*waaW*	*B6N50_00430* →	-	UDP-galactose--(galactosyl) LPS alpha1,2-galactosyltransferase	79,820	c→t	Q281stop	Rough	Easy	1
R35	*galU*	*B6N50_13325* ←	-	UTP--glucose-1-phosphate uridylyltransferase	2,611,872 - 2,611,880	INS 2,783,815 - 2,784,945	S75_L78ins(377)	Deep rough	Hard	2

141

Table S1: List of mutations found in *E. coli* C strains that are resistant to wildtype ΦX174. *E. coli* C resistant strains: R# is the strain number. Genes: name of the gene(s) in which mutations have been identified (as compared with wildtype *E. coli* C; doi: 10.5281/zenodo.6952399). Locus tags: identifier of each listed gene. Synonyms: alternative gene names. Descriptions: protein product encoded by each listed gene. Positions: genomic coordinates of mutation. Nucleotide changes: observed nucleotide change. Amino acid changes: resulting change in amino acid sequence. Predicted LPS structure phenotypes: based on predicted LPS structure (see **Fig. 2**). "Easy" or "Hard" LPS structure phenotypes?: easy LPS phenotypes were overcome or could be cross-infected after the first phage evolution experiment, while hard LPS phenotypes required the second or third phage evolution experiment to be infected. "INS": insertion. "DUP": duplication. "stop": stop codon. "[a]": L249fsTer#263 indicates a frameshift (fs) leading to a premature codon stop (Ter); the position of the premature stop codon is in parentheses. "[b]": M168_V172ins(376) indicates an insertion; the two flanking amino acids are separated by a "_" and followed by the number of inserted amino acids in parentheses. "[c]": Δ[EutM_A58-EutE_A181] indicated a long deletion starting from EutM to EutE. P242_A276dup(34) indicates a duplication; the two flanking amino acids are separated by a "_" and followed by the number of duplicated amino acids in parentheses.

ΦX174 strains	Evolution experiment #	Gene mutated in the corresponding *E. coli* C resistant strains	Mutants sensitive to the evolved ΦX174 strain infection	Gene mutated in ΦX174 strains	Descriptions	Positions	Nucleotide changes	Amino acid changes	Are mutations present in a control lineage?
R21 T1	1	*waaO*	R5, R4, R13, R20, R21, R24, R29, WT	*F*	Capsid protein	1,347	a→g	D116G	No
				H	Minor spike protein	3,132	g→a	A68T	No
R24 T1	1	*waaO*	R5, R4, R13, R20, R21, R24, R29, WT	*F*	Capsid protein	1,346	g→a	D116S	No
				F	Capsid protein	1,347	a→g	D116S	No
R26 T1	1	*bldE*	R18, R8, R10, R26, R12, R7, R4, R13, R20, R21, R24, R29	*F*	Capsid protein	1,460	c→a	Q154K	No
				H	Minor spike protein	3,132	g→a	A68T	No
R27 T1	1	*bldE*	R27, R31, WT	*H*	Minor spike protein	3,202	g→t	G91V	No
R29 T1	1	*waaO*	R5, R4, R13, R20, R21, R24, R29, WT	*F*	Capsid protein	1,346	g→a	D116S	No
				F	Capsid protein	1,347	a→g	D116S	No
R31 T1	1	*bldE*	R27, R31, WT	*H*	Minor spike protein	3,202	g→t	G91V	No
R18 T4	1	*waaC*	R18, R8, R10, R26, R12, R14, R4, R13, R20, R21, R24, R29	*F*	Capsid protein	1,307	t→c	Y103H	No
				F	Capsid protein	1,461	a→g	Q154R	No
				H	Minor spike protein	3,132	g→a	A68T	No
R20 T5	1	*waaO*	R5, R27, R31, R12, R14, R4, R13, R20, R21, R24, R29, WT	*F*	Capsid protein	1,354	t→a	N118K	No
				H	Minor spike protein	3,132	g→a	A68T	No
R8 T6	1	*bldE*	R18, R8, R10, R26, R12, R14, R4, R13, R20, R21, R24, R29	*F*	Capsid protein	1,307	t→c	Y103H	No
				F	Capsid protein	1,461	a→g	Q154R	No
				F	Capsid protein	3,132	g→a	A68T	No
R10 T6	1	*bldE*	R18, R8, R10, R26, WT	*F*	Capsid protein	1,317	a→g	H106R	No

				F	Capsid protein	1,460	c→a	Q154K	No
R13 T6	1	*waaO*	R11, R4, R13, R20, R21, R24, R29, R33, R2, R34, WT	*F*	Capsid protein	2,015	g→c	D339H	No
R4 T7	1	*waaO*	R4, R13, R20, R21, R24, R29, WT	*F*	Capsid protein	1,301	a→g	T101A	Yes (in C1 T21)
				F	Capsid protein	1,347	a→g	D116G	No
				F	Capsid protein	2,085	c→t	A362V	No
R22 T1	2	*galU*	R18, R8, R10, R26, R32, R12, R14, R16, R17, R30, R35, R22, R28, R23, R9, R7, R4, R13, R20, R21, R24, R29	*F*	Capsid protein	1,307	t→c	Y103H	No
				F	Capsid protein	1,317	a→g	H106R	No
				F	Capsid protein	1,461	a→g	Q154R	No
				H	Minor spike protein	3,132	g→a	A68T	No
R28 T1	2	*waaG*	R18, R8, R10, R26, R32, R12, R14, R16, R17, R30, R35, R22, R28, R23, R9, R7, R4, R13, R20, R21, R24, R29	*F*	Capsid protein	1,307	t→c	Y103H	No
				F	Capsid protein	1,317	a→g	H106R	No
				F	Capsid protein	1,461	a→g	Q154R	No
				H	Minor spike protein	3,132	g→a	A68T	No
R25 T4	3	*rfaH*	R5, R18, R8, R10, R26, R12, R14, R25, R11, R7, R4, R13, R20, R21, R24, R29, R33, R2, R34, WT	*F*	Capsid protein	1,301	a→g	T101A	Yes (in C1 T21)
				F	Capsid protein	1,304	g→c	G102R	No
				F	Capsid protein	1,347	a→g	D116G	No
				H	Minor spike protein	3,132	g→a	A68T	No
R6 T12	3	*waaP*	R5, R18, R27, R31, R32, R6, R4, R13, R20, R21, R24, R29, R2, R34, WT	*F*	Capsid protein	1,727	c→t	L243F	No
				F	Capsid protein	2,015	g→c	D339H	No
				H	Minor spike protein	3,132	g→a	A68T	No
				H	Minor spike protein	3,154	c→t	A75V	No

155

156 **Table S2: List of mutations identified in ΦX174 evolved isolates.** ΦX174 strains: R# is the corresponding resistant strain number and
157 T# is the transfer number where plaques were observed for the first time on the given resistant strain. Evolution experiment #: experiment
158 number from which the evolved phages were isolated. Mutants sensitive to the evolved ΦX174 strains infection: list of all resistant strains
159 that a specific phage strain can infect (See **Figs. 6 and S3**). Descriptions: names of proteins encoded by the listed genes. Positions: genomic
160 coordinates of mutation (according to GenBank accession number AF176034.1). Nucleotide changes: observed nucleotide change. Amino
161 acid changes: resulting change in amino acid sequence. Are mutations present in a control lineage?: indicates mutations that were observed
162 in at least one control lineage (see **Methods**).
163

ΦX174 populations	Gene mutated in the corresponding *E. coli* C resistant strains	Gene mutated in ΦX174 strains	Descriptions	Positions	Nucleotide changes	Amino acid changes	Frequencies (%)	Are mutations present in a control lineage?
C1 T21	None (WT)	*F*	Capsid protein	1,301	a→g	T101A	69,8	-
		F	Capsid protein	1,965	g→a	G322D	70,9	-
C2 T21	None (WT)	*F*	Capsid protein	1,968	a→g	N323S	17,8	-
		F	Capsid protein	2,277	c→t	T426I	56,7	-
C3 T21	None (WT)	*F*	Capsid protein	2,277	c→t	T426I	5,7	-
		F	Capsid protein	2,280	c→t	S247L	80,7	-
R2 T21	*waaW*	*F*	Capsid protein	1,965	g→a	G322D	19,0	Yes (in C1 T21)
		F	Capsid protein	2,276	a→g	T426A	30,4	No
		F	Capsid protein	2,279	t→c	S427P	10,9	No
		F	Capsid protein	2,280	c→t	S247L	30,9	Yes (in C3 T21)
R5 T21	*gmhB*	NA	NA	NA	NA	NA	NA	NA
R7 T21	*waaO*	*F*	Capsid protein	2,279	t→c	S427P	5,4	
		F	Capsid protein	2,280	c→t	S247L	93,2	Yes (in C3 T21)
R9 T21	*waaG*	*F*	Capsid protein	2,280	c→t	S247L	100	Yes (in C3 T21)
R11 T21	*waaP*	NA	NA	NA	NA	NA	NA	NA
R12 T21	*waaF*	*F*	Capsid protein	2,280	c→t	S247L	100	Yes (in C3 T21)
R14 T21	*waaF*	*F*	Capsid protein	2,280	c→t	S247L	93,5	Yes (in C3 T21)
R16 T21	*galU*	*F*	Capsid protein	2,280	c→t	S247L	100	Yes (in C3 T21)
R17 T21	*galU*	*F*	Capsid protein	2,279	t→c	S427P	6,7	No
		F	Capsid protein	2,280	c→t	S247L	93,1	Yes (in C3 T21)

R23 T21	*waaG*	*F*	Capsid protein	1,301	a→g	T101A	5,6	Yes (in C1 T21)
		F	Capsid protein	2,280	c→t	S247L	91,6	Yes (in C3 T21)
R30 T21	*galU*	*F*	Capsid protein	2,279	t→c	S427P	7,9	No
		F	Capsid protein	2,280	c→t	S247L	90,0	Yes (in C3 T21)
R32 T21	*bldE*	*F*	Capsid protein	2,276	a→g	T426A	29,6	No
		F	Capsid protein	2,277	c→t	T426I	6,8	Yes (in C2 T21 and C3 T21)
		F	Capsid protein	2,280	c→t	S247L	61,9	Yes (in C3 T21)
R33 T21	*waaT*	*F*	Capsid protein	2,276	a→g	T426A	42,9	No
		F	Capsid protein	2,277	c→t	T426I	14,8	Yes (in C2 T21 and C3 T21)
		F	Capsid protein	2,280	c→t	S247L	41,7	Yes (in C3 T21)
		*A/A**	Replication-associated protein/protein A*	4,817	c→t	D279D/D107D	12,8	No
R34 T21	*waaW*	NA	NA	NA	NA	NA	NA	NA
R35 T21	*galU*	*F*	Capsid protein	1,301	a→g	T101A	19,1	Yes (in C1 T21)
			Capsid protein	1,649	c→t	R217C	8,0	No
			Capsid protein	2,179	g→t	Q393H	6,8	No
			Capsid protein	2,280	c→t	S247L	82,9	Yes (in C3 T21)

164 **Table S3: List of mutations found in the evolved ΦX174 populations that did not infect their corresponding *E. coli* C resistant**
165 **strains.** ΦX174 populations: R# is the corresponding resistant strain number and T# is the transfer number where plaques were observed
166 for the first time on the given resistant strain. Descriptions: names of proteins encoded by the listed genes. Positions: genomic coordinates
167 of mutation (according to GenBank accession number AF176034.1). Nucleotide changes: observed nucleotide change. Amino acid changes:

168 resulting change in amino acid sequence. Frequencies (%): frequency of a given mutation in the phage population. Are mutations present in
169 a control lineage?: indicates mutations that were observed in at least one control lineage (see **Methods**). NA: no data available.
170

Excluded *E. coli* C resistant strains	Genes	Locus tags	Synonyms	Descriptions	Positions	Nucleotide changes	Amino Acid changes	Predicted LPS structure phenotypes
R1	*waaV*	*B6N50_00435* →	-	UDP-glucose:(Glucosyl) LPS β1,3-Glucosyltransferase	80,534	$(t)_{7\rightarrow 6}$	F149fsTer#158[a]	Rough
	galE	*B6N50_15815* →	-	UDP-glucose 4-epimerase	3,096,098 - 3,096,107	Δ10 bp	T228fsTer#233	
R3	*galE*	*B6N50_15815* →	-	UDP-glucose 4-epimerase	3,095,443	g→a	G10D	Rough
R15	*galE*	*B6N50_15815* →	-	UDP-glucose 4-epimerase	3,096,191	c→a	Y259stop	Rough
R19	*yajC*	*B6N50_17610* ←	-	Preprotein translocase subunit	3,447,574	Δ1 bp	G18fsTer#23	Wildtype

ΦX174 strains	Evolution experiment #	Gene mutated in the corresponding *E. coli* C resistant strains	Gene mutated in ΦX174 strains	Descriptions	Positions	Nucleotide changes	Amino acid changes	Are mutations present in a control lineage?
R19 T1	1	*yajC*	*H*	Minor spike protein	3,781	c→a	S284Y	No
R5 T2	1	*gmhB*	*H*	Minor spike protein	3,169	c→t	G80V	No

Table S4: List of all *E. coli* C and evolved ΦX174 isolates excluded from the analysis. *E. coli* C resistant strains: R# is the excluded resistant strain number. Genes: name of gene(s) in which mutations have been identified (as compared with wildtype *E. coli* C; doi: 10.5281/zenodo.6952399). Locus tags: identifier of each listed gene. Synonyms: alternative gene names. Descriptions: protein product encoded by each listed gene. Positions: genomic coordinates of mutation. Nucleotide changes: observed nucleotide change. Amino acid changes: resulting change in amino acid sequence. Predicted LPS structure phenotypes: based on predicted LPS structure (see **Fig. 2**). "stop": stop codon. "[a]": F149fsTer#158 indicates a frameshift (fs) leading to a premature codon stop (Ter); the position of the premature stop codon is in parentheses. ΦX174 strains: R# is the corresponding resistant strain number and T# is the transfer number where plaques were observed for the first time on the given resistant strain. Evolution experiment #: experiment number where the evolved phages were obtained.

180 Descriptions: names of proteins encoded by the listed genes. Positions: genomic coordinates of mutation (according to GenBank accession
181 number AF176034.1). Nucleotide changes: observed nucleotide change. Amino acid changes: resulting change in amino acid sequence. Are
182 mutations present in a control lineage?: indicates mutations that were observed in at least one control lineage (see **Methods**).
183

E. coli C resistant strains	Replicate #	Genes	Locus tags	Descriptions	Positions	Nucleotide changes	Amino Acid changes	Predicted LPS structure phenotypes
R3	1	*gltD*	*B6N50_02830* ←	Glutamate synthase subunit gltD	555,954	t→c	Y318C	Rough
		galE	*B6N50_15815* →	UDP-glucose 4-epimerase	3,095,443	g→a	G10D	
R3	2, 3, 5, 9, 10	*WaaT*	*B6N50_00420* →	UDP-galactose:(glucosyl) LPS α-1,2-galactosyltransferase	77,302	$(a)_{6\rightarrow5}$	K16fsTer#23[a]	Rough
		gltD	*B6N50_02830* ←	Glutamate synthase subunit gltD	555,954	t→c	Y318C	
		-	-	Hypothetical protein	2,147,627	c→t	Q793stop	
		galE	*B6N50_15815* →	UDP-glucose 4-epimerase	3,095,443	g→a	G10D	
R3	4	*oppB*	*B6N50_13280* ←	Murein tripeptide ABC transporter/inner membrane subunit	2,600,004	g→a	A211V	Deep rough
		galU	*B6N50_13325* ←	UTP--glucose-1-phosphate uridylyltransferase	2,611,933	Δ1 bp	I57fsTer#86	
		galE	*B6N50_15815* →	UDP-glucose 4-epimerase	3,095,443	g→a	G10D	
R3	6	*gmhD*	*B6N50_00455* ←	ADP-L-glycero-D-mannoheptose-6-epimerase	84,986	g→t	Y140stop	Rough
		galE	*B6N50_15815* →	UDP-glucose 4-epimerase	3,095,443	g→a	G10D	
R3	7	*galE*	*B6N50_15815* →	UDP-glucose 4-epimerase	3,095,443	g→a	G10D	Rough
		galT	*B6N50_15820* →	Galactose-1-phosphate uridylyltransferase	3,097,396	t→c	L319P	
R3	8	*gltD*	*B6N50_02830* ←	Glutamate synthase subunit gltD	555,954	t→c	Y318C	Rough
		-	-	Hypothetical protein	2,147,627	c→t	Q793stop	
		galE	*B6N50_15815* →	UDP-glucose 4-epimerase	3,095,443	g→a	G10D	
R15	1	*galP*	*B6N50_04295* ←	Galactose-proton symporter	835,258	a→g	F405L	Rough
		galE	*B6N50_15815* →	UDP-glucose 4-epimerase	3,096,191	c→a	Y259stop	

R15	2	*WaaT*	*B6N50_00420* →	UDP-galactose:(glucosyl) LPS α-1,2-galactosyltransferase	77,590	g→t	E112stop	Rough
		galE	*B6N50_15815* →	UDP-glucose 4-epimerase	3,096,191	c→a	Y259stop	
R15	3 - 6	*waaW*	*B6N50_00430* →	UDP-galactose--(galactosyl) LPS alpha1,2-galactosyltransferase	79,764	t→g	L262R	Rough
		galE	*B6N50_15815* →	UDP-glucose 4-epimerase	3,096,191	c→a	Y259stop	
R15	7	*galP*	*B6N50_04295* ←	Galactose-proton symporter	836,442	g→t	S10stop	Rough
		galE	*B6N50_15815* →	UDP-glucose 4-epimerase	3,096,191	c→a	Y259stop	
R15	8	*galP*	*B6N50_04295* ←	Galactose-proton symporter	835,353	a→g	L373P	Rough
		galE	*B6N50_15815* →	UDP-glucose 4-epimerase	3,096,191	c→a	Y259stop	
R15	9	*galE*	*B6N50_15815* →	UDP-glucose 4-epimerase	3,096,191	c→a	Y259stop	Rough
R15	10	*galP*	*B6N50_04295* ←	Galactose-proton symporter	835,170	c→t	W434stop	Rough
		galE	*B6N50_15815* →	UDP-glucose 4-epimerase	3,096,191	c→a	Y259stop	

Table S5: List of the additional mutations associated with *galE* mutations. *E. coli* C resistant strains: R# is the resistant strain number. Genes: name of the gene(s) in which mutations have been identified (as compared with wildtype *E. coli* C; doi: 10.5281/zenodo.6952399). Locus tags: identifier of each listed gene. Descriptions: protein product encoded by each listed gene. Positions: genomic coordinates of mutation. Nucleotide changes: observed nucleotide change. Amino acid changes: resulting change in amino acid sequence. Predicted LPS structure phenotypes: based on predicted LPS structure (see **Fig. 2**). "stop": stop codon. "[a]": K16sTer#23 indicates a frameshift (fs) leading to a premature codon stop (Ter); the position of the premature stop codon is in parentheses.

Name	Sequence (5'→3')	Binding Region	Tm 2Q5	Ta 2Q5	Purpose
ΦX174_2361_r	TCGCTTGGTCAACCCCTCAG	2342-2361	70˚C	71˚C	ΦX174 Whole genome amplification
ΦX174_2362_f	AGCGCGGTAGGTTTTCTGCT	2362-2382	70˚C		
ΦX174_399_r	CTTGACTCATGATTTCTTACC	379-399	58˚C	59˚C	ΦX174 Whole genome amplification
ΦX174_400_f	TTACTGAACAATCCGTACGTTTC	400-422	62˚C		

Name	Sequence (5'→3')	Binding Region	Tm Phusion (buffer HF)	Ta Phusion (buffer HF)	Purpose
ΦX174_F_fw	CGCTCGTCTTTGGTATGTAGGTGG	928-951	65˚C	68˚C	Amplification of ΦX174's *F* gene
ΦX174_F_rv	AGCGGCGTTGACAGATGTATCC	2580-2601	65˚C		Amplification of ΦX174's *F* gene
ΦX174_F_fw2	GTTGCGAGGTACTAAAGGCAAGCG	898-921	66˚C	68˚C	Amplification of ΦX174's *F* gene
ΦX174_F_rv2	CTGGAGTAACAGAAGTGAGAACCAGC	2245-2470	65˚C		Amplification of ΦX174's *F* gene
ΦX174_F_fw_sh	CGTCTTTGGTATGTAGGTGG	932-951	57˚C	61˚C	Amplification of ΦX174's *F* gene
ΦX174_F_rv_sh	CGGCGTTGACAGATGTATC	2581-2599	58˚C		Amplification of ΦX174's *F* gene
ΦX174_H_fw	CAAGGACTGTGTGACTATTGACGTCC	2763-2788	65˚C	68˚C	Amplification of ΦX174's *H* gene
ΦX174_H_rv	GCCTCTACGCGATTTCATAGTGGAG	4490-4514	65˚C		Amplification of ΦX174's *H* gene
ΦX174_H_fw2	CGCTACTAAATGCCGCGGATTGG	2847-2869	66˚C	67˚C	Amplification of ΦX174's *H* gene
ΦX174_H_rv2	GCCTCCAGCAATCTTGAACACTC	4467-4489	64˚C		Amplification of ΦX174's *H* gene
ΦX174_H_fw_sh	GACTGTGTGACTATTGACGTCC	2767-2788	60˚C	61˚C	Amplification of ΦX174's *H* gene
ΦX174_H_rv_sh	GCCTCTACGCGATTTCATAG	4495-4514	58˚C		Amplification of ΦX174's *H* gene

Name	Sequence (5'→3')	Binding Region	Tm	Ta	Purpose
ΦX174_F_Sanger_fw	CCTCATCGTCACGTTTATGG	1217-1236	58°C	56°C	Sanger sequencing of ΦX174's *F* gene
ΦX174_F_Sanger_fw2	ACCGATATTGCTGGCGAC	1934-1951	59°C	56°C	Sanger sequencing of ΦX174's *F* gene
ΦX174_F_Sanger_rv	GGCGTTATAACCTCACACTC	2294-2313	58°C	56°C	Sanger sequencing of ΦX174's *F* gene
ΦX174_F_Sanger_rv2	GGCGAGAAAGCTCAGTCTC	1529-1547	60°C	56°C	Sanger sequencing of ΦX174's *F* gene
ΦX174_H_Sanger_fw	GTGGCGCCATGTCTAAATTG	2974-2993	59°C	56°C	Sanger sequencing of ΦX174's *H* gene
ΦX174_H_Sanger_fw2	CAGCAAACGCAGAATCAGC	3720-3738	60°C	56°C	Sanger sequencing of ΦX174's *H* gene
ΦX174_H_Sanger_rv	CCACAAGCCTCAATAGCAG	4054-4072	58°C	56°C	Sanger sequencing of ΦX174's *H* gene
ΦX174_H_Sanger_rv2	CTTTATCAGCGGCAGACTTG	3251-3270	58°C	56°C	Sanger sequencing of ΦX174's *H* gene

191

192 **Table S6. List of primers used in this study.** *F*: encodes for the viral capsid protein. *H*: encodes for the minor spike protein. "fw": forward.
193 "rv": reverse**.** Tm 2Q5: melting temperature of the primer used with the Q5® High-Fidelity 2X Master Mix (NEB). Ta 2Q5: annealing
194 temperature of the set of primers used with the Q5® High-Fidelity 2X Master Mix (NEB). Tm Phusion (buffer HF): melting temperature of
195 the primer used with Phusion® High-Fidelity PCR Master Mix with HF Buffer (ThermoFisher). Ta Phusion (buffer HF): annealing
196 temperature of the primer used with Phusion® High-Fidelity PCR Master Mix with HF Buffer (ThermoFisher).

197 **Supplementary Methods**

198

199 In this section, we provide a more detailed version of the protocols used in the **Methods** section.

200

201 **First phage evolution experiment - Standard**. The protocol from Bono *et al.* (Bono et al. 2012)
202 was adapted to evolve phages that can infect resistant *E. coli* C strains. Of R1-R35 – the 35 *E. coli*
203 C strains resistant to ΦX174 wildtype, see above – 31 were used for the first phage evolution
204 experiment (excluding R1, R3, R15, and R19; see **Results** and **Text S1**). Thirty-one ΦX174
205 lineages were each founded by ΦX174 wildtype and serially transferred daily, for up to 21 days,
206 on non-evolving host cultures containing a mix of (i) *E. coli* C wildtype (permissive strain) and (ii)
207 one resistant *E. coli* C strain (non-permissive strain; R2-R35).

208

209 For each transfer, permissive and non-permissive bacteria were grown separately until they reached
210 the log phase. These cultures were founded with an initial inoculum of 180 μl from fast and
211 intermediate growers' overnight cultures or 350 μl from slow growers' overnight cultures (see **Fig.**
212 **S4**). Fast and intermediate growers' cultures were incubated at 37°C (250 rpm) for two hours, while
213 slow growers' cultures were incubated for three hours. Then, permissive and non-permissive
214 strains were mixed in a 14 ml sterile tube at a specific ratio depending on the growth of the non-
215 permissive strain (1:1 for fast growers, 1:2 for intermediate growers, 1:3 for slow growers), to a
216 final volume of 5 ml.

217

218 At each transfer, ~10^8 freshly prepared susceptible cells were infected by ~10^7 ΦX174 (MOI_{input}
219 ~0.1). Infected cultures were shaken at 250 rpm, 37°C for three hours. Phage lysates were isolated
220 as described in **Phage lysate preparation**. Phage lysates from the previous day were used to
221 inoculate the fresh bacterial mixes the next day. Transfers continued until phages were found to
222 infect their corresponding resistant *E. coli* C strain, or until 21 transfers were reached. Three control
223 lines were also run in parallel, by transferring ΦX174 at MOI_{input} ~0.1 in a culture containing *E.*
224 *coli* C wildtype (permissive strain) only.

225

226 **Second phage evolution experiment – Increased diversity.** A phage cocktail made of (i) the
227 wildtype ΦX174 and (ii) all ΦX174 strains that successfully re-infected their corresponding
228 resistant strains during the phage evolution experiment – Standard was generated by first diluting
229 each phage lysate and mixing them at a roughly equal number of pfu (final concentration of ~2.10^8
230 pfu ml^{-1}). These phage strains (14 in total) are: ΦX174 R4 T7, ΦX174 R5 T2, ΦX174 R8 T6,

231 ΦX174 R10 T6, ΦX174 R13 T6, ΦX174 R18 T4, ΦX174 R19 T1, ΦX174 R20 T5, ΦX174 R21
232 T1, ΦX174 R24 T1, ΦX174 R26 T1, ΦX174 R27 T1, ΦX174 R29 T1, and ΦX174 R31 T1.
233 Despite being removed from the mutational analysis, phages infecting R5 and R19, respectively,
234 were part of the final cocktail (see **Text S1** and **Table S4**).
235
236 The phage cocktail was grown and transferred daily, for up to four days, on non-evolving host
237 cultures containing: (i) *E. coli* C wildtype, (ii) the 14 host strains for which resistance had been
238 overcome (permissive hosts: *E. coli* C R4, R5, R8, R10, R13, R18, R19, R20, R21, R24, R26, R27,
239 R29, and R31), and (iii) an excess of one of the still-resistant strain of interest (non-permissive
240 host). For the non-permissive host, we used R6 (*waaP/pssA* mutant), R22 (*galU* mutant), R25 (*rfaH*
241 mutant), or R28 (*waaG* mutant; see **Table S1**). *E. coli* C R22 and R28 were chosen as representatives
242 of the *galU* and *waaG* mutants, respectively.
243
244 Each bacterial strain (permissive and non-permissive) was grown separately in LB liquid culture
245 for one hour (37°C, 250 rpm). An inoculum of 180 μl from overnight cultures was used for the
246 fast and intermediate growers, while 350 μl was used for the slow growers. After the incubation
247 time, permissive strains were pooled at a roughly equal number of colony-forming units (CFU),
248 for a final concentration of ~10^8 susceptible, permissive cells. One of the *E. coli* C resistant strains
249 of interest (non-permissive host; R6, R22, R25 or R28) was then added in excess (in between ~1
250 and $5x10^8$ resistant cells) in the host mix, to give a final volume of 4 ml.
251
252 Infections were initiated by adding ~10^7 phages (MOI_{input} ~0.1) from the phage cocktail to the
253 bacterial culture mix. Infected cultures were shaken in 100 ml sterile Erlenmeyer at 250 rpm, 37°C,
254 for five hours. Phage lysates were isolated as described in **Phage lysate preparation**. Phage lysates
255 from the previous day were used to inoculate the fresh bacterial mixes the next day. This process
256 was repeated until phages were found to infect their corresponding resistant *E. coli* C strains, or
257 until four transfers had been completed.
258
259 **Third evolution experiment – Increased diversity and generations.** The same phage cocktail
260 used in the second phage evolution experiment – Increased diversity was grown and transferred
261 daily, four times a day, for up to four days on non-evolving host cultures containing (i) *E. coli* C
262 wildtype, (ii) the 14 host strains for which resistance had been overcome (permissive hosts: *E. coli*
263 C R4, R5, R8, R10, R13, R18, R19, R20, R21, R24, R26, R27, R29, and R31), and (iii) one of the
264 still-resistant strain of interest (non-permissive host). The definitive protocol from the second

265 phage evolution experiment – Increased diversity was adjusted to reduce the amount of time
266 necessary to retrieve the desired phages. We increased the number of transfers per day from one
267 to four for a total of four days (16 transfers in total). Only *E. coli* C R6 (*waaP*/*pssA* mutant) and
268 R25 (*rfaH* mutant) (see **Table S1**) were used as non-permissive hosts.
269
270 Each bacterial strain (permissive and non-permissive) was grown separately for one hour. An
271 inoculum of 180 µl from overnight cultures was used for the fast and intermediate growers, while
272 350 µl was used for the slow growers. After the incubation time, permissive strains were pooled
273 at a roughly equal number of colony-forming units (CFU) in three different mixes depending on
274 the growth categories of each bacterium (slow, intermediate, and fast growers, **Fig. S4**). 1 ml of
275 each fast grower was used to make the "fast mix" (constituted of *E. coli* C wildtype, R5, R19, R27,
276 and R31). 833 µl of each intermediate grower was used for the "intermediate mix" (constituted of
277 R4, R13, R20, R21, R24, and R29). Finally, 1.25 ml of each slow grower was used to prepare the
278 "slow mix" (constituted of R8, R10, R18, and R26).
279
280 Non-permissive strains and bacterial mixes were kept in exponential growth phase independently
281 by transferring 1:5 of the volume (1 ml) in fresh LB pre-heated at 37°C every hour (final volume
282 of 5 ml). To check whether the growth of the different bacteria remained consistent from one
283 transfer to another, the OD600 values were measured before each transfer. The volume
284 transferred at each hour was modified accordingly if the bacterial growth was too fast or too slow.
285
286 Before adding the phage cocktail, all bacterial mixes were pooled together at a roughly equal
287 number of cfu (500 µl each, for a total of ~10^8 susceptible cells), and one of the *E. coli* C resistant
288 strains of interest (non-permissive host; R6 or R25) was added in excess (i.e., the number of
289 resistant cells was comprised between ~1 and 5.10^8), for a final volume of 4 ml.
290
291 Infections started by adding ~10^7 phages (MOI_{input} ~0.1) from the cocktail in the final bacterial
292 mix. Infected cultures were shaken in 100 ml sterile Erlenmeyer at 250 rpm, 37°C, for one hour.
293 After that, 1:15 of the volume of each infected culture was transferred to freshly mixed bacterial
294 cultures and the infection continued for one hour. This step was repeated for a total of four
295 transfers. The final (fourth) transfer lasted for two hours to ensure that all phages completed the
296 infection cycle and are present in the culture medium and not in the cell. All transfers completed
297 on the same day involved transferring both phage and bacteria; on every fourth transfer,
298 supernatants were collected and only phages were transferred. Phage lysates were isolated as

299 described in **Phage lysate preparation**. Phage lysates from the previous day were used to
300 inoculate the first fresh bacterial mixes the next day. This entire process was repeated until phages
301 that could infect their corresponding resistant *E. coli* C strains were identified or until four transfers
302 had been completed.
303
304 **Isolation of evolved ΦX174 strains from single plaques.** To isolate pure, single clones from
305 the different evolution experiments, top agar overlays were prepared by mixing 100 µl of undiluted
306 phage lysates with 200 µl of an overnight culture of the corresponding resistant *E. coli* C strain in
307 4 ml SSA (supplemented with $CaCl_2$ and $MgCl_2$ at a final concentration of 5 and 10 mM,
308 respectively). Top agar overlays were poured onto LB plates, dried for at least 15 minutes, and
309 incubated inverted at 37˚C for ~16-17 hours. Plaques were counted the next day. An isolated
310 plaque was chosen randomly for each phage lysate to infect cultures of the corresponding resistant
311 *E. coli* C strains (in exponential growth state) incubated at 37˚C, 250 rpm, for five hours. Phage
312 lysates were isolated as described in **Phage lysate preparation**. To obtain pure phage glycerol
313 stocks (isogenic stocks which are presumed to hold one genetic clone (van Charante et al. 2019)),
314 phages were purified via a second round of plaque isolation from their first glycerol stocks. Phage
315 lysates were isolated and stored as described in **Phage lysate preparation**.
316
317 **Determination of the evolved phages' host range by spotting assays**
318 *Method 1*. Each top agar overlay was prepared by mixing 200 µl of an *E. coli* C strain from stationary
319 phase culture in 4 ml SSA (supplemented with $CaCl_2$ and $MgCl_2$ at a final concentration of 5 and
320 10 mM, respectively), then poured on LB plates and dried for at least 15 minutes under a sterile
321 laminar flow hood. Then, 3 µl of each undiluted evolved phage lysate (between 10^7 and 10^9 pfu
322 ml^{-1}) was dropped at the surface.
323
324 *Method 2*. Each top agar overlay was prepared by mixing a volume of each phage lysate in 4 ml SSA
325 at a final concentration of ~10^7 pfu ml^{-1}, then poured on LB plates and dried for at least 15 minutes
326 under a sterile laminar flow hood. Then, 3 µl of both undiluted and ten-fold diluted of each *E. coli*
327 C strain (from overnight culture) were dropped onto the surface with a pipette.
328
329 For both methods, spots were dried for at least 30 minutes under sterile laminar flow, and the
330 plates were subsequently incubated inverted at 37˚C for ~17 hours. *E. coli* C wildtype was used as
331 a positive control (permissive strain), and *E. coli* K-12 MG1655 as a negative control (non-
332 permissive strain). Sterile H_2O was also spotted at the end of each plate as a control for material

333 contamination (pipettes and tips). A bacterial host strain was classified as sensitive only when signs
334 of lysis were detected using both methods, in at least two (of three) replicates per method. A phage-
335 bacterium combination that yielded different results between the two methods was tested in
336 *standard plaque assays* as follows: a top agar overlay was prepared by mixing 100 μl of the phage
337 lysate diluted to 10^{-1} and 10^{-6} with 200 μl of the resistant *E. coli* C strain from stationary phase
338 culture in 4 ml SSA supplemented with $CaCl_2$ and $MgCl_2$ at a final concentration of 5 and 10 mM,
339 respectively), then poured on LB plates and dried for at least 15 minutes. The presence or absence
340 of plaques was assessed the next day. Finally, the host strain was classified as sensitive if plaques
341 were observed at both dilutions.
342
343

344 **References**

345 Amor K, Heinrichs DE, Frirdich E, Ziebell K, Johnson RP, Whitfield C. 2000. Distribution of
346 core oligosaccharide types in lipopolysaccharides from *Escherichia coli*. *Infect Immun.*
347 68:1116–1124.

348 Belunis CJ, Clementz T, Carty SM, Raetz CRH. 1995. Inhibition of lipopolysaccharide biosynthesis
349 and cell growth following inactivation of the *kdtA* gene in *Escherichia coli*. *J Biol Chem.*
350 270:27646–27652.

351 Bohm K, Porwollik S, Chu W, Dover JA, Gilcrease EB, Casjens SR, McClelland M, Parent KN.
352 2018. Genes affecting progression of bacteriophage P22 infection in *Salmonella* identified
353 by transposon and single gene deletion screens: host genes affecting phage P22 infection.
354 *Mol Microbiol.* 108:288–305.

355 Bono LM, Gensel CL, Pfennig DW, Burch CL. 2012. Competition and the origins of novelty:
356 experimental evolution of niche-width expansion in a virus. *Biol Lett.* 9:20120616–
357 20120616.

358 van Charante F, Holtappels D, Blasdel B, Burrowes B. 2019. Isolation of bacteriophages. In:
359 Harper DR, Abedon ST, Burrowes BH, McConville ML, editors. Bacteriophages: Biology,
360 Technology, Therapy. Springer, Cham. p. 1–32.

361 Fang J, Wei Y. 2011. Expression, purification and characterization of the *Escherichia coli* integral
362 membrane protein YajC. *Protein Pept Lett.* 18:601–608.

363 Frey PA. 1996. The Leloir pathway: a mechanistic imperative for three enzymes to change the
364 stereochemical configuration of a single carbon in galactose. *FASEB j.* 10:461–470.

365 Genevaux P, Bauda P, DuBow MS, Oudega B. 1999. Identification of Tn10 insertions in the *rfaG*,
366 *rfaP*, and *galU* genes involved in lipopolysaccharide core biosynthesis that affect *Escherichia*
367 *coli* adhesion. *Arch of Microbiol.* 172:1–8.

368 Hancock RE, Reeves P. 1976. Lipopolysaccharide-deficient, bacteriophage-resistant mutants of
369 *Escherichia coli* K-12. *J Bacteriol.* 127:98–108.

370 Heinrichs DE, Yethon JA, Amor PA, Whitfield C. 1998. The assembly system for the outer core
371 portion of R1- and R4-type lipopolysaccharides of *Escherichia coli*: the R1 core-specific β-
372 glucosyltransferase provides a novel attachment site for O-polysaccharides. *J Biol Chem.*
373 273:29497–29505.

374 Heinrichs DE, Yethon JA, Whitfield C. 1998. Molecular basis for structural diversity in the core
375 regions of the lipopolysaccharides of *Escherichia coli* and *Salmonella enterica*. *Mol Microbiol.*
376 30:221–232.

377 Jansson P-E, Lindberg B, Lindberg AA, Wollin R. 1981. Structural studies on the hexose region
378 of the core in lipopolysaccharides from Enterobacteriaceae. *Eur J Biochem.* 115:571–577.

379 Karp PD, Billington R, Caspi R, Fulcher CA, Latendresse M, Kothari A, Keseler IM,
380 Krummenacker M, Midford PE, Ong Q, et al. 2019. The BioCyc collection of microbial
381 genomes and metabolic pathways. *Brief Bioinform.* 20:1085–1093.

382 Kawaura T, Inagaki M, Karita S, Kato M, Nishikawa S, Kashimura N. 2000. Recognition of
383 receptor lipopolysaccharides by spike G protein of bacteriophage ΦX174. *Biosci Biotechnol*
384 *Biochem.* 64:1993–1997.

385 Klein G, Lindner B, Brabetz W, Brade H, Raina S. 2009. *Escherichia coli* K-12 suppressor-free
386 mutants lacking early glycosyltransferases and late acyltransferases: minimal

387 lipopolysaccharide structure and induction of envelope stress response. *J Biol Chem.*
388 284:15369–15389.

389 Klein G, Müller-Loennies S, Lindner B, Kobylak N, Brade H, Raina S. 2013. Molecular and
390 structural basis of inner core lipopolysaccharide alterations in *Escherichia coli*: incorporation
391 of glucuronic acid and phosphoethanolamine in the heptose region. *J Biol Chem.* 288:8111–
392 8127.

393 Kneidinger B, Marolda C, Graninger M, Zamyatina A, McArthur F, Kosma P, Valvano MA,
394 Messner P. 2002. Biosynthesis pathway of ADP-L-glycero-β-D-manno-heptose in
395 *Escherichia coli. J. Bacteriol.* 184:363-369.

396 Król JE, Hall DC, Balashov S, Pastor S, Sibert J, McCaffrey J, Lang S, Ehrlich RL, Earl J, Mell JC,
397 et al. 2019. Genome rearrangements induce biofilm formation in *Escherichia coli* C – an old
398 model organism with a new application in biofilm research. *BMC Genomics* 20:767.

399 Kulikov EE, Golomidova AK, Prokhorov NS, Ivanov PA, Letarov AV. 2019. High-throughput
400 LPS profiling as a tool for revealing of bacteriophage infection strategies. *Sci Rep.* 9:2958.

401 Labrie SJ, Samson JE, Moineau S. 2010. Bacteriophage resistance mechanisms. *Nat Rev Microbiol.*
402 8:317–327.

403 Leipold MD, Vinogradov E, Whitfield C. 2007. Glycosyltransferases involved in biosynthesis of
404 the outer core region of *Escherichia coli* lipopolysaccharides exhibit broader substrate
405 specificities than is predicted from lipopolysaccharide structures. *J Biol Chem.* 282:26786–
406 26792.

407 van der Ley P, de Graaff P, Tommassen J. 1986. Shielding of *Escherichia coli* outer membrane
408 proteins as receptors for bacteriophages and colicins by O-antigenic chains of
409 lipopolysaccharide. *J Bacteriol* 168:449–451.

410 Matsuura M. 2013. Structural modifications of bacterial lipopolysaccharide that facilitate Gram-
411 Negative bacteria evasion of host innate immunity. *Front Immunol.* 109:4.

412 McArthur F, Andersson CE, Loutet S, Mowbray SL, Valvano MA. 2005. Functional analysis of
413 the glycero-manno-heptose 7-phosphate kinase domain from the bifunctional HldE
414 protein, which is involved in ADP-L-glycero-D-manno-heptose biosynthesis. *J Bacteriol.*
415 187:5292–5300.

416 Mutalik VK, Adler BA, Rishi HS, Piya D, Zhong C, Koskella B, Kutter EM, Calendar R,
417 Novichkov PS, Price MN, et al. 2020. High-throughput mapping of the phage resistance
418 landscape in *E. coli. PLoS Biol.* 18:e3000877.

419 Pagnout C, Sohm B, Razafitianamaharavo A, Caillet C, Offroy M, Leduc M, Gendre H, Jomini S,
420 Beaussart A, Bauda P, et al. 2019. Pleiotropic effects of *rfa*-gene mutations on *Escherichia*
421 *coli* envelope properties. *Sci Rep.* 9:9696.

422 Pierson DE, Carlson S. 1996. Identification of the *galE* gene and a *galE* homolog and
423 characterization of their roles in the biosynthesis of lipopolysaccharide in a serotype O:8
424 strain of *Yersinia enterocolitica. J Bacteriol.* 178:5916–5924.

425 Raetz CRH, Whitfield C. 2002. Lipopolysaccharide endotoxins. *Annu Rev Biochem.* 71:635–700.

426 Schnaitman CA, Austin EA. 1990. Efficient incorporation of galactose into lipopolysaccharide by
427 *Escherichia coli* K-12 strains with polar *galE* mutations. *J Bacteriol.* 172:5511–5513.

428 Schnaitman CA, Klena JD. 1993. Genetics of lipopolysaccharide biosynthesis in enteric bacteria.
429 *Microbiol Rev.* 57:655–682.

430 Schulze RJ, Komar J, Botte M, Allen WJ, Whitehouse S, Gold VAM, Nijeholt JAL a, Huard K,
431 Berger I, Schaffitzel C, et al. 2014. Membrane protein insertion and proton-motive-force-
432 dependent secretion through the bacterial holo-translocon SecYEG–SecDF–YajC–YidC.
433 *PNAS* 111:4844–4849.

434 Vinogradov EV, van der Drift K, Thomas-Oates JE, Meshkov S, Brade H, Holst O. 1999. The
435 structures of the carbohydrate backbones of the lipopolysaccharides from *Escherichia coli*
436 rough mutants F470 (R1 core type) and F576 (R2 core type): LPS from *E. coli* R1 and R2
437 core types. *Eur J Biochem.* 261:629–639.

438 Weissborn AC, Liu Q, Rumley MK, Kennedy EP. 1994. UTP:α-D-glucose-L-phosphate
439 uridylyltransferase of *Escherichia coli*: isolation and DNA Sequence of the *galU* gene and
440 purification of the enzyme. *J Bacteriol.* 176:2611-2618.

441 Whitfield C, Heinrichs DE, Yethon JA, Amor KL, Monteiro MA, Perry MB. 1999. Assembly of
442 the R1-type core oligosaccharide of *Escherichia coli* lipopolysaccharide. *J Endotoxin Res.*
443 5:151–156.

444 Yethon JA, Heinrichs DE, Monteiro MA, Perry MB, Whitfield C. 1998. Involvement of *waaY*,
445 *waaQ*, and *waaP* in the modification of *Escherichia coli* lipopolysaccharide and their role in
446 the formation of a stable outer membrane. *J Biol Chem.* 273:26310–26316.

447 Yethon JA, Vinogradov E, Perry MB, Whitfield C. 2000. Mutation of the lipopolysaccharide core
448 glycosyltransferase encoded by *waaG* destabilizes the outer membrane of *Escherichia coli* by
449 interfering with core phosphorylation. *J Bacteriol.* 182:5620–5623.

450